Molecular Pharmacology Fast Forward. Published on October 18, 2010 as doi:10.1124/mol.110.069062
This article has not been copyedited and formatted. The final version may differ from this version.

Iron Chelators of the DpT and BpT Series Inhibit HIV-1 Transcription: Identification of Novel Cellular Targets – Iron, CDK2 and CDK9

Zufan Debebe, Tatyana Ammosova, Denitra Breuer, David B. Lovejoy, Danuta S. Kalinowski, Pradeep K. Karla, Krishna Kumar, Marina Jerebtsova, Patricio Ray, Fatah Kashanchi, Victor R. Gordeuk, Des R. Richardson[1] and Sergei Nekhai[1]

Center for Sickle Cell Disease, Department of Medicine, Howard University, Washington DC (Z.D., T.A., D.B., V.R.G., S.N.); Department of Pharmaceutical Sciences, Howard University, Washington DC (Z.D., P.K.K., K.K); Department of Microbiology, Howard University, Washington DC (D.B., S.N.); Iron Metabolism and Chelation Program, Department of Pathology and Bosch Institute, University of Sydney, Sydney, Australia (D.B.L., D.S.K., D.R.R.); Children's National Medical Center, Washington, D.C. (M.J., P.R.) and National Center for Biodefense and Infectious Diseases, George Mason University, Manassas, VA (F.K.)

Molecular Pharmacology Fast Forward. Published on October 18, 2010 as DOI: 10.1124/mol.110.069062
This article has not been copyedited and formatted. The final version may differ from this version.

a) Running Title: Iron Chelators Inhibit HIV-1 Transcription

b) Corresponding author: Des R. Richardson, Iron Metabolism and Chelation Program, Department of Pathology and Bosch Institute, Blackburn Building (D06), University of Sydney, Sydney, New South Wales, 2006 Australia; Telephone: +61-2-9036-6548 ; Fax: 9351-3429; E-mail: d.richardson@med.usyd.edu.au

c) Text pages - 46

Tables - 1

Figures – 8

Supplemental Figures - 2

References - 40

Abstract words - 239

Introduction words – 611

Discussion words –1,485

d) A list of non-standard abbreviations used in the paper: CDK2, cyclin-dependent kinase 2; CDK9, cyclin-dependent kinase 9; Tat, HIV-1 transcription activation protein; DpT, di-2-pyridylketone thiosemicarbazone; BpT, 2-benzoylpyridine thiosemicarbazone; ARC, 4-amino-6-hydrazino-7-beta-D-ribofuranosyl-7H-pyrroloF-pyrimidine-5-carboxamide; LTR, Long terminal repeat.

Molecular Pharmacology Fast Forward. Published on October 18, 2010 as DOI: 10.1124/mol.110.069062
This article has not been copyedited and formatted. The final version may differ from this version.

Abstract

HIV-1 transcription is activated by HIV-1 Tat protein, which recruits CDK9/cyclin T1 and other host transcriptional co-activators to the *HIV-1* promoter. Tat itself is phosphorylated by cyclin-dependent kinase 2 (CDK2) and inhibition of CDK2 by siRNA or the iron chelators, 311 or ICL670, inhibits HIV-1 transcription. Here we have analyzed a group of novel di-2-pyridylketone thiosemicarbazone (DpT) and 2-benzoylpyridine thiosemicarbazone (BpT)-based iron chelators that exhibit marked anti-cancer activity *in vitro* and *in vivo* (Whitnall M, Howard J, Ponka P and Richardson DR (2006) *Proc Natl Acad Sci USA* 103:7670-5; Kalinowski DS, Yu Y, Sharpe PS, Islam M, Liao Y-T, Lovejoy DB, Kumar N, Bernhardt PV and Richardson DR. (2007) *J Med Chem* 50:3716-29). Several of these iron chelators, in particular Bp4aT and Bp4eT, inhibited HIV-1 transcription and replication at much lower concentrations than 311 and ICL670. Both Bp4aT and Bp4eT were not toxic after a 24 h incubation. However, longer incubations for 48 h or 72 h resulted in cytotoxicity. Analysis of the molecular mechanism of HIV-1 inhibition showed that the novel iron chelators inhibited basal HIV-1 transcription, but not the NF-κB-dependent transcription or transcription from a *HIV-1* promoter with inactivated SP1 sites. The chelators inhibited the activities of CDK2 and cyclin-dependent kinase 9 (CDK9)/cyclin T1, suggesting that inhibition of CDK9 may contribute to the inhibition of HIV-1 transcription. Our study suggests the potential usefulness of Bp4aT or Bp4eT in anti-retroviral regimens, particularly where resistance to standard treatment occurs.

Molecular Pharmacology Fast Forward. Published on October 18, 2010 as DOI: 10.1124/mol.110.069062
This article has not been copyedited and formatted. The final version may differ from this version.

Introduction

Increased iron stores are correlated with faster HIV-1 progression in iron-loaded thalassemia major patients, in HIV-positive patients administered with oral iron and those with the haptoglobin 2-2 polymorphism (Gordeuk et al., 2001). Moreover, a retrospective study of bone marrow macrophage iron in HIV-positive patients suggested that survival was inversely correlated with higher iron stores (Gordeuk et al., 2001).

Iron chelation therapy has been considered for the control of various infections such as those mediated by protozoa or intracellular pathogens (Hershko, 1994). Several studies have demonstrated the potential of iron chelators in inhibiting HIV replication (Georgiou et al., 2002; Georgiou et al., 2000; Traore and Meyer, 2004). In cultured T cells, excess iron stimulates HIV-1 viral replication, whereas iron chelation with desferrioxamine (DFO) lowers viral replication, as measured by decreased p24 levels and reverse transcriptase (RT) activity (Traore and Meyer, 2004). Treatment of monocyte-derived macrophages and peripheral blood lymphocytes with the chelators, DFO or deferiprone (CP20), reduced p24 expression and inhibited cellular proliferation (Georgiou et al., 2000). The orally-active bidentate chelators, CP502 and CP511, decreased HIV-1 replication and cellular proliferation in a manner similar to DFO and CP20 (Georgiou et al., 2002). Thus, the observed reduction of HIV-1 replication by these chelators may reflect inhibition of cellular proliferation, rather than inhibition of a specific host cell factor involved in HIV-1 replication.

Molecular Pharmacology Fast Forward. Published on October 18, 2010 as DOI: 10.1124/mol.110.069062
This article has not been copyedited and formatted. The final version may differ from this version.

In our previous study, HIV-1 transcription was inhibited in CEM T cells by the tridentate iron chelators, 2-hydroxy-1-naphthylaldehyde isonicotinoyl hydrazone (311, IC_{50} = 2 μM) and ICL670 (also known as deferasirox, IC_{50} = 23 μM) (Debebe et al., 2007). These iron chelators inhibited the cellular activity of cyclin-dependent kinase 2 (CDK2) (Debebe et al., 2007). While ICL670 has been recently approved for clinical use in the United States and has been successfully implemented for the treatment of iron overload (Porter, 2006), the relatively high concentrations of ICL670 needed for the inhibition of HIV-1 was of concern. The iron chelator, 311, was shown to be cytotoxic at low micromolar concentrations (IC_{50} = 3 μM) (Becker et al., 2003). Hence, the inhibition of HIV-1 that we observed with 311 may be partly related to the inhibition of DNA synthesis and cellular proliferation.

The goal of the present study was to screen and identify novel iron chelators that would be more potent inhibitors of HIV-1 transcription than ICL670 or equally inhibitory but less cytotoxic than 311. We also were interested to determine whether inhibition of HIV-1 transcription was due to the inhibition of cyclin-dependent kinase 9 **(**CDK9)/cyclin T1, a major RNA polymerase II kinase that interacts with HIV-1 Tat and induces HIV-1 transcription (Nekhai and Jeang, 2006). For this purpose, we examined a library of di-2-pyridylketone thiosemicarbazone (DpT) and 2-benzoylpyridine thiosemicarbazone (BpT)-based tridentate iron chelators (Fig. 1A) (Kalinowski et al., 2007; Whitnall et al., 2006; Yuan et al., 2004). The DpT chelators and especially di-2-pyridylketone-4,4-dimethyl-3-thiosemicarbazone (Dp44mT), have been shown to have potent anti-tumor activity *in vitro* and *in vivo* (Whitnall et al., 2006; Yuan et al., 2004). Notably, mice

Molecular Pharmacology Fast Forward. Published on October 18, 2010 as DOI: 10.1124/mol.110.069062
This article has not been copyedited and formatted. The final version may differ from this version.

treated with optimal Dp44mT doses showed little alteration in hematological and biochemical indices at the chelator doses (0.4 mg/kg/day) required to induce anti-tumor activity (Whitnall et al., 2006). The BpT-based iron chelators exhibited comparable anti-neoplastic activity than their DpT homologs *in vitro* and are amongst the most active anti-cancer agents developed by Richardson and colleagues (Kalinowski et al., 2007).

In the current investigation, we identified the two most potent inhibitors of HIV-1 from the BpT and DpT series of chelators and discovered novel molecular mechanisms involved in their activity. Utilization of these new iron chelating agents in treatment schedules could be of clinical significance in HIV patients with drug resistance to current anti-viral treatment regimens.

Molecular Pharmacology Fast Forward. Published on October 18, 2010 as DOI: 10.1124/mol.110.069062
This article has not been copyedited and formatted. The final version may differ from this version.

Materials and Methods

Materials.

293T and CEM T cells were purchased from the American Type Culture Collection (ATCC; Manassas, VA). The CEM-HIV-1 (LTR) GFP cells (courtesy of Dr. Jacques Corbeil) and OM10.1 cells (courtesy of Dr. Salvatore Butera) were obtained from the NIH AIDS Research and Reference Reagent Program. Histone H1 was purchased from Upstate Cell Signaling Solutions (Charlottesville, VA). Anti-FLAG monoclonal antibody, protein G and protein A agarose were purchased from Sigma (Atlanta, GA). All radioactive reagents were purchased from GE Health Care Life Sciences (Piscataway, NJ). Antibodies against CDK9, CDK2 and cyclin T1 were purchased from Santa Cruz Biotechnology (Santa Cruz, CA). Horseradish peroxidase (HRP)-conjugated $F(ab)_2$ fragment was purchased from Amersham Biosciences (Piscataway, NJ). All other inorganic reagents were purchased from Fisher Scientific (Fair Lawn, NJ) or Sigma (St. Louis, MO). Roscovitin was purchased from Calbiochem (La Jolla, CA) and 4-amino-6-hydrazino-7-beta-D-ribofuranosyl-7H-pyrrolo[2,3-d]-pyrimidine-5-carboxamide (ARC) was a gift from Dr. Andrei Gartel (University of Illinois, IL).

Chelators.

All chelators were synthesized by Schiff base condensation between the relevant aromatic ketone or aldehyde with a thiosemicarbazide or acid hydrazide using standard methods (Kalinowski et al., 2007). The chelators were characterized using a combination of elemental analysis, ^{1}H-NMR spectroscopy, infrared spectroscopy and mass spectroscopy.

Molecular Pharmacology Fast Forward. Published on October 18, 2010 as DOI: 10.1124/mol.110.069062
This article has not been copyedited and formatted. The final version may differ from this version.

Cell culture.

All cells were cultured at 37°C in a 5% CO_2 atmosphere. CEM T cells and peripheral blood mononuclear cells (PBMCs) were cultured in Roswell Park Memorial Institute 1640 (RPMI) medium (Invitrogen, Rockville, MD) containing 10% fetal bovine serum (FBS) and 1% antibiotic solution (penicillin and streptomycin; Invitrogen). CEM GFP cells were cultured in RPMI medium with all the additions above, but also 500 μg/mL G418 (Invitrogen). The 293T cells and OM10.1 cells were cultured in Dulbecco's Modified Eagle's Medium (DMEM; Invitrogen) containing 10% FBS and 1% antibiotic solution (penicillin and streptomycin).

Induction of HIV-1 transcription with Ad-Tat.

The E1-deleted recombinant Adeno virus carrying Tat was generated as previously described (Debebe et al., 2007). Briefly, CEM-GFP cells were infected in 96-well plates containing 400,000 cells/well. After 24 h at 37°C, 10 μL aliquots were removed, supplemented with trypan blue and counted to determine cellular viability. The remaining cells were transferred to a white plate (Perkin-Elmer, Waltham, MA) and fluorescence was measured at 480 nm excitation and 510 nm emission using a LS50B luminescence spectrometer (Perkin-Elmer).

Data analysis.

Cytotoxicity data are presented as a percentage of the control versus logarithm of the chelator concentration and analyzed using GraphPad Prism 3 software (GraphPad Software, La Jolla, CA). The IC_{50} values were determined from the dose-response

Molecular Pharmacology Fast Forward. Published on October 18, 2010 as DOI: 10.1124/mol.110.069062
This article has not been copyedited and formatted. The final version may differ from this version.

(variable slope) curve using a four parameter logistic equation, namely: Y=Bottom+(Top-Bottom)/(1+1^(logEC50-X)*Hill Slope).

Plasmids.

The HIV-1 reporter containing HIV-1 long terminal repeat (LTR; -138 to +82) followed by a nuclear localization signal (NLS) and the *LacZ* reporter gene (courtesy of Dr. Michael Emmerman, Fred Hutchinson Cancer Institute, Seattle, WA) and the pNL4-3.Luc.R$^-$E$^-$ (Courtesy of Prof. Nathaniel Landau, NYU School of Medicine, New York, NY) were obtained from the NIH AIDS Research and Reference Reagent Program. The NF-κB driven *e-selectin-luciferase* reporter was a gift from Dr. Chou-Zen Giam (Uniformed Services University of the Health Sciences, Bethesda, Maryland) (Fu et al., 2003). The following plasmids were kindly provided by Dr. Manuel López-Cabrera (Unidad de Biología Molecular, Madrid, Spain): WT HIV-1 LTR (-105 to +77) followed by the *luciferase* reporter gene (KB SP WT); HIV-1 (-105 to +77) with Sp1-inactivated sites followed by the *luciferase* reporter gene (WT SP 123); and HIV-1 (-81 to +77) with NF-κB-deleted sites followed by the *luciferase* reporter gene.

Transient transfections.

293T cells were co-transfected with Tat-expressing vector and HIV-1 LTR-*LacZ* at 30% confluence using Lipofectamine and Plus reagents (Invitrogen, Rockville, MD) and the indicated reporter plasmids. After transfection, the cells were cultured for an additional 48 h at 37^{o}C and β-galactosidase activity was analyzed using the quantitative *o*-

Molecular Pharmacology Fast Forward. Published on October 18, 2010 as DOI: 10.1124/mol.110.069062
This article has not been copyedited and formatted. The final version may differ from this version.

nitrophenyl-β-D-galactopyranoside (ONPG)-based assay (see below) (Debebe et al., 2007).

β-galactosidase assays.

Cells were washed with PBS and lysed for 20 min at room temperature in 50 µL of lysis buffer, containing 20 mM HEPES at pH 7.9, 0.1% NP-40 and 5 mM EDTA. Subsequently, 100 µL of ONPG solution (72 mM Na_2PO_4 at pH 7.5, 1 mg/mL ONPG, 12 mM $MgCl_2$, 180 mM 2-mercaptoethanol) was added and incubated at room temperature. Standards were incubated for 10 min. Based on the linear part of the standard curve, the color development was monitored and stopped when the signal was in the middle of the linear range. The reaction was terminated by the addition of 100 µL of 1 M Na_2CO_3. The 96-well plate was analyzed in a microplate reader at 414 nm (Lab Systems Multiscan MS; Vienna, VA).

Cell viability assays (propidium iodide uptake, calcein-AM uptake and trypan blue exclusion assay).

CEM T cells were grown in 96-well plates at 37°C and incubated with iron chelators for the indicated period of time. To measure toxicity by propidium iodide (PI, Sigma) uptake, PI (250 µg/mL) was incubated with cells for 30 min at 37°C. PI fluorescence was measured at 488 nm excitation and 617 nm emission using the luminescence spectrometer described above.

To assess cytotoxicity with calcein, media was removed and the cells washed with *D*-

Molecular Pharmacology Fast Forward. Published on October 18, 2010 as DOI: 10.1124/mol.110.069062
This article has not been copyedited and formatted. The final version may differ from this version.

PBS in order to remove serum esterase activity that may cause an increase in fluorescence through the hydrolysis of calcein-AM. Cells were then supplemented with 0.2 μM calcein-AM (Molecular Probes, Invitrogen) for 10 min at 37°C. A positive control containing 100% dead cells was prepared by treating cells with Triton X-100 (1% v/v) which were then incubated with 0.2 μM calcein-AM. Fluorescence was measured using the luminescence spectrometer described above implementing 495 nm excitation and 515 nm emission filters.

To measure cellular viability, the cells were supplemented with 0.2% trypan blue, transferred to a plastic disposable counting chamber and counted on a Cellometer Automatic Cell Counter (Nexcelcom Bioscience, Lawrence, MA).

Preparation of pseudotyped HIV-1 virus expressing luciferase.

293T cells were grown on 100 mm plates at 37°C and transfected using the calcium phosphate method. Cells were transfected with the VSVG-expressing vector (gpHEF-VSVG) and pNL4-3.Luc.R-E- molecular clone that contains two nonsense frame shifts in the *Env* and *Vpr* genes. In this vector, the *luciferase* gene was cloned in place of *nef* (He and Landau, 1995). After 72 h post-transfection, the media was collected, briefly centrifuged at 1,000 x*g* for 10 min and the virus collected by centrifugation at 4°C for 6 h at 14,000 x*g*. The precipitated virus was resuspended in PBS containing 10% glycerol, aliquoted and stored at –70°C. The p24 analysis of the HIV-1 Luc was performed by ELISA using a kit from ZeptoMetrix (Buffalo, NY).

Molecular Pharmacology Fast Forward. Published on October 18, 2010 as DOI: 10.1124/mol.110.069062
This article has not been copyedited and formatted. The final version may differ from this version.

Luciferase assay.

CEM T cells were infected with VSVG-pseudotyped pNL4-3.Luc.R-E-virus and then cultured at 0.5 x 10^6 cells/mL in 6-well plates at 37°C and 5% CO_2. The cells were collected, washed with PBS and resuspended in 100 µL of PBS. Then, 100 µL of reconstituted luciferase buffer (Luclite Kit, Perkin Elmer) was added to each well and after 10 min incubation, the lysates were transferred into white plates (Perkin Elmer) and luminescence measured using Labsystems Luminoscan RT equipment (Perkin Elmer).

Source of peripheral blood mononuclear cells (PBMCs).

PBMCs were purchased from Astarte Biologics (Redmond, WA). Donors were negative for HIV-1 and -2, hepatitis B, hepatitis C and HTLV-1. PBMCs were isolated from peripheral blood by apheresis with additional purification by density gradient centrifugation and cryopreserved until used.

Infection of PBMCs with VSVG HIV-Luc and inhibition of HIV-1 with iron chelators.

PBMCs were infected with VSVG-pseudotyped pNL4-3.Luc.R-E- (HIV-1 Luc) virus at approximately 1 ng of p24 per 5 x 10^6 cells. The virus was prepared as described above. After 48 h, the cells were seeded on 96 well white plates and incubated with the iron chelators for 24 h/37^{o}C. Then, luciferase buffer was added to each well and luminescence measured using Labsystems Luminoscan RT equipment, as described above.

Molecular Pharmacology Fast Forward. Published on October 18, 2010 as DOI: 10.1124/mol.110.069062
This article has not been copyedited and formatted. The final version may differ from this version.

Viability of PBMC after iron chelator treatment.

PBMCs were grown on a 96-well white plate and incubated with the iron chelators for different time periods at 37^{o}C. Later, cells were washed with PBS, incubated with 0.2 μM calcein-AM for 15 min and fluorescence measured at an excitation of 495 nm and an emission of 515 nm using Luminescence Spectrometer LS50B. Values presented are mean ± SD (n = 4) and are typical of 3 independent experiments.

Inhibition of HIV-1 replication using iron chelators.

In these studies, OM10.1 cells were used where the integrated HIV-1 proviral DNA was originally derived from the subtype B, LAI strain (Butera et al., 1994). To assess the activity of chelators on inhibiting HIV-1 replication, 1 x 10^6 OM10.1 cells were grown to 70% confluency and treated with 10 ng/mL TNF-α for 2 h at 37^{o}C. Subsequently, TNF-α was removed, the cells washed with PBS and then treated with the indicated concentrations of iron chelators. Media was collected 48 h after the drug treatment and the activity of reverse transcriptase (RT) determined. Viral supernatants (10 μL) were incubated in a 96-well plate with RT reaction mixture containing 1x RT buffer (50 mM Tris-HCl, 1 mM DTT, 5 mM $MgCl_2$, 20 mM KCl), 0.1% Triton, poly(A) (10^{-2} U), poly(dT) (10^{-2} U) and (^{3}H)TTP. The mixture was incubated overnight at 37°C and 5 μL of the reaction mix was spotted on a DEAE filtermat, washed four times with 5% Na_2HPO_4 and three times with water and then dried completely. RT activity was measured using a Betaplate counter (Perkin Elmer).

Molecular Pharmacology Fast Forward. Published on October 18, 2010 as DOI: 10.1124/mol.110.069062
This article has not been copyedited and formatted. The final version may differ from this version.

Analysis of the NF-κB driven e-selectin-luciferase reporter activity.

293T cells were seeded at 30% confluence in 96-well plates and allowed to grow overnight. The following day, the cells were transfected with CMV-EGFP reporter in combination with the NF-κB driven *e-selectin-luciferase* reporter (Fu et al., 2003), or pNL4-3.Luc.R$^-$E$^-$ (*HIV-1* promoter) for 3 h at 37^{o}C using lipofectamine and then incubated with Bp4aT or Bp4eT for 48 h at 37^{o}C. The media was then removed from the cells and equal amounts of PBS and luciferase buffer were added to measure luciferase activity. Following luciferase activity, GFP was measured at an excitation of 495 nm and an emission of 515 nm.

Analysis of HIV-1 promoters with the deletion of NF-κB and inactivation of Sp1 sites.

293T cells were transfected at 30% confluency in 96-well plates with vectors in which the *luciferase* reporter was driven by WT HIV-1 LTR (-105 to +77), HIV-1 LTR (-105 to +77) with Sp1-inactivated sites or HIV-1 LTR (-81 to +77) with NF-κB-deleted sites (courtesy of Dr. Manuel López-Cabrera, Unidad de Biología Molecular, Madrid, Spain). The cells were transfected for 3 h at 37^{o}C using Lipofectamine and Plus and then incubated with iron chelators or control medium for 18 h at 37^{o}C. The media was then removed from the cells and equal amounts of 1x PBS and luciferase buffer were added to measure luciferase activity.

Immunoblots and kinase assay.

293T cells were incubated with control medium or this medium containing chelators and incubated for 24 h at 37°C. Cells were then washed with PBS and whole-cell lysates were

Molecular Pharmacology Fast Forward. Published on October 18, 2010 as DOI: 10.1124/mol.110.069062
This article has not been copyedited and formatted. The final version may differ from this version.

prepared from the cells using whole cell lysis buffer (50 mM Tris-HCl, pH 7.5, 0.5 M NaCl, 1% NP-40, 0.1% SDS) supplemented with anti-protease cocktail (Sigma). Protein concentration of the lysates was measured by the Bradford assay (Bio-Rad, Hercules, CA) and 30-50 μg of total protein was subjected to electrophoresis using 10% SDS-PAGE. The gels were transferred onto PVDF membrane (Millipore, Allen, TX) and analyzed for CDK2, CDK9 and cyclin T1. The blots were developed and quantified using a ChemiDoc XRS Station (Bio-Rad). Immunoprecipitations were carried out with 400 μg of the cell lysate and 800 ng of antibody combined with 50 μL of a 50% slurry of protein A agarose for 2 h at 4°C in a TNN buffer (50 mM Tris-HCl, pH 7.5, 0.15 M NaCl and 1% NP-40). The agarose beads were precipitated, washed with TNN buffer and divided into two parts and used for the kinase assay and western blotting. The kinase assay was performed at 30^{o}C for 30 min in a kinase assay buffer (50 mM HEPES-KOH, pH 7.9, 10 mM $MgCl_2$, 6 mM EGTA, 2.5 mM DTT) containing 1 μg of histone H1 as a substrate, 200 μM cold ATP and 5 μCi of (γ-^{32}P) ATP.

C-Terminal domain (CTD) of RNA polymerase II phosphorylation assay.

The CTD phosphorylation assay was performed at 30^{o}C for 30 min in 20 μL of kinase assay buffer (50 mM HEPES-KOH, pH 7.9, 10 mM $MgCl_2$, 6 mM EGTA, 2.5 mM DTT) containing 4 μg of CTD substrate, 250 μM cold ATP and 5 μCi of (γ-^{32}P) ATP. Recombinant CDK2/cyclin E or CDK9/cyclin T1 were used as controls. The reaction was stopped with SDS-loading buffer and resolved using 10% PAGE. The dried gel was exposed to a Phosphor imager screen. In parallel, the products of immunoprecipitation were resolved using 10% Tris-Glycine SDS-PAGE, transferred to polyvinylidene fluoride

Molecular Pharmacology Fast Forward. Published on October 18, 2010 as DOI: 10.1124/mol.110.069062
This article has not been copyedited and formatted. The final version may differ from this version.

(PVDF) membranes (Millipore, Allen, TX) and immunoblotted with appropriate antibodies.

Separation of large and small CDK9/cyclin T1-containing complexes by differential salt extraction.

We used a method developed by Price and colleagues to quantify the relative amounts of the large and small CDK9/cyclin T1-containing complexes based on differential nuclear extraction (Biglione et al., 2007). 293T cells were grown on 6 well plates at 37°C and 5% CO_2 and then incubated with the iron chelators (1 μM) for 24 h at 37°C. Cells were then suspended in buffer A (10 mM Hepes (pH 7.9), 10 mM KCl, 10 mM $MgCl_2$, 1 mM EDTA, 250 μM sucrose, 1 mM DTT, 0.5% NP-40 and protease inhibitors cocktail (Sigma)) added at 500 μL/10^7 cells. The mixture was incubated on ice for 10 min and centrifuged at 1000 x*g* for 5 min to pellet the nucleus. The supernatant was removed and saved as the low salt extract (LS). The remaining pellet was resuspended in Buffer B (20 mM Hepes-KOH (pH 7.9), 450 mM NaCl, 1.5 mM $MgCl_2$, 0.5 mM EDTA, 1 mM DTT and protease inhibitors cocktail) added at 500 μL/10^7 cells. The mixture was incubated on ice for 10 min and centrifuged at 10,000 x*g* for 1 h/4^{o}C. The supernatant was collected as the high salt extract (HS) and the pellet was discarded. The lysates were loaded on 10% polyacrylamide gel and transferred to PVDF membrane and western blotting analysis was performed for the expression of CDK9 and cyclin T1.

Molecular Pharmacology Fast Forward. Published on October 18, 2010 as DOI: 10.1124/mol.110.069062
This article has not been copyedited and formatted. The final version may differ from this version.

Statistical analysis.

Results were expressed as mean ± standard deviation. Data were compared using Student's *t*-test. Results were considered significant when $p < 0.05$.

Molecular Pharmacology Fast Forward. Published on October 18, 2010 as DOI: 10.1124/mol.110.069062
This article has not been copyedited and formatted. The final version may differ from this version.

Results

Identification of Bp4aT and Bp4eT as the most efficient and least cytotoxic inhibitors of HIV-1 transcription.

We analyzed 15 selected DpT and BpT-derived iron chelators including a control non-chelating analogue, Dp2mT, that was designed and characterized in previous studies (Kalinowski et al., 2007; Yuan et al., 2004) (Fig. 1A and Table 1). These agents were assessed using CEM-T cells containing an integrated HIV-1 LTR–GFP (CEM-GFP). HIV-1 transcription in CEM-GFP cells was induced by infection with adenovirus expressing Tat (Ad-Tat) and GFP fluorescence was measured to quantify viral transcription, as previously described (Debebe et al., 2007; Nekhai et al., 2007). Data were analyzed using GraphPad Prism 3 software and showed that after a 24 h incubation of CEM T cells with the fifteen chelators tested, eleven ligands inhibited HIV-1 transcription with sub-micromolar IC_{50} values (Table 1 and Fig. 1, panels B and C). The six most active chelators (IC_{50}<0.2 μM) were Dp44mT, Dp4pT, Bp44mT, Bp4eT, Bp4aT and Bp4pT (Table 1). Bp44mT had the lowest IC_{50} for inhibition of HIV-1 transcription, namely 15 nM (Table 1 and Fig. 1C).

The short-term toxicity of the iron chelators was analyzed by propidium iodide uptake in the treated CEM T cells in comparison to the untreated control. As a positive control for cell death, untreated cells were lysed by the addition of the non-ionic detergent, Triton X-100 (1% v/v). Toxicity of the chelators and that of the non-cytotoxic, non-chelating control compound, Dp2mT (Yuan et al., 2004), were then analyzed. These results showed that Dp4pT, Bp44mT, Bp4pT and PKTBH were clearly cytotoxic over 24 h (see IC_{50}

Molecular Pharmacology Fast Forward. Published on October 18, 2010 as DOI: 10.1124/mol.110.069062
This article has not been copyedited and formatted. The final version may differ from this version.

values in Table 1 and Supplemental Fig. 1). As shown previously, Dp2mT was not cytotoxic at concentrations below 10 μM, as it cannot bind cellular iron pools (Yuan et al., 2004).

Inhibition of one-round HIV-1 replication in CEM T cells.

Based on the results above, we selected Bp4aT and Bp4eT for further analysis as the most potent and least cytotoxic compounds that inhibited HIV-1 transcription in 293T and CEM T cells. We analyzed the effect of Bp4aT and Bp4eT on one round of HIV-1 replication in comparison to the positive and negative controls, Bp4pT and BpT, that showed marked or little activity in inhibiting HIV-1 transcription, respectively (Table 1). In these experiments, CEM T cells were infected with pseudotyped HIV-1 virus containing luciferase in place of the *nef* gene (HIV-1 Luc) (He and Landau, 1995). CEM T cells were infected overnight with the virus and then cultured for 24 h at 37^{o}C with or without the indicated concentration of chelators (Fig. 2A). In these experiments, Bp4eT was the most efficient inhibitor (IC_{50} = 75.0 ± 5.5 nM), followed by Bp4aT (IC_{50} = 160 ± 16 nM), Bp4pT (IC_{50} = 340 ± 53 nM) and BpT (IC_{50} = 1.60 ± 0.26 μM) (Fig. 2A).

Inhibition of one-round HIV-1 replication in PBMCs.

We also analyzed the effect of Bp4aT and Bp4eT on one-round of HIV-1 replication in PBMCs in comparison to BpT. PBMCs were infected with pseudotyped HIV-1 Luc virus for 48 h at 37°C and then cultured for 24 h at 37°C with or without the indicated concentration of chelators (Fig. 2B). In these cells, only Bp4aT markedly inhibited

Molecular Pharmacology Fast Forward. Published on October 18, 2010 as DOI: 10.1124/mol.110.069062
This article has not been copyedited and formatted. The final version may differ from this version.

luciferase activity with an IC_{50} = 25 nM, whereas Bp4eT inhibited HIV-1 replication at a much higher concentration (IC_{50} = 1.3 μM; Fig. 2B).

Inhibition of HIV-1 replication in OM10.1 cells.

Considering the effective anti-viral activity observed above on HIV-1 transcription or one-round HIV-1 replication, it was important to compare the efficacy of the most effective chelators on productive HIV-1 replication. To perform these studies, we utilized HIV-1-infected OM10.1 cells that were treated with TNF-α to analyze the inhibitory effects of iron chelators. Both Bp4eT and Bp4aT inhibited HIV-1 replication with the IC_{50} being 2.4 $\pm$ 0.4 μM and 6.4 $\pm$ 2.7 μM, respectively (Fig. 2C). Thus, the chelators were also able to inhibit productive HIV-1 replication.

Comparison of the inhibition of HIV-1 transcription by Bp4aT and Bp4eT to that of ARC and roscovitin.

Considering the effective anti-viral activity observed above, it was important to compare the efficacy of the most effective chelators with known HIV-1 transcription inhibitors. We compared inhibition of HIV-1 transcription in 293T cells transfected with HIV-1 LTR-LacZ and Tat expression vectors. Bp4aT and Bp4eT inhibited Tat-induced HIV-1 transcription in 293T cells at low micromolar concentrations (Fig. 3A). To compare the effect of the iron chelators to the effect of known HIV-1 transcription inhibitors, we incubated these transfected cells with ARC or roscovitin which inhibit HIV-1 transcription through the de-regulation of CDK9 and CDK2, respectively (reviewed in (Nekhai and Jeang, 2006)). After a 24 h incubation at 37°C, HIV-1 transcription was

Molecular Pharmacology Fast Forward. Published on October 18, 2010 as DOI: 10.1124/mol.110.069062
This article has not been copyedited and formatted. The final version may differ from this version.

inhibited by ARC (IC_{50} =180 nM) and by roscovitin (IC_{50} = 1.5 μM) (Fig. 3B). Thus, the iron chelators, Bp4aT and Bp4eT, were approximately 4-16 times less efficient inhibitors of HIV-1 than ARC, but comparable to roscovitin. However, it is relevant to note that these chelators have not been specifically designed as anti-viral agents and their potential may lie in their novel mechanism of action (examined below).

Toxicity of iron chelators.

Analysis of short-term cytotoxicity of Bp4aT and Bp4eT was performed in comparison to the negative control chelator, BpT, that showed little toxicity after 24 h (Table 1). In these studies using calcein-AM uptake (Papadopoulos et al., 1994), the chelators were demonstrated to be equally non-toxic after a 24 h incubation period (IC_{50} >100 μM, Fig. 4A). We further analyzed long-term cytotoxicity of Bp4aT and Bp4eT in comparison to the negative control BpT in CEM T cells after 1-5 days of incubation implementing the calcein-AM assay. The number of viable cells decreased after 2 days treatment and remained low for up to 5 days of incubation (Fig. 4B). Analysis of cell growth using the trypan blue viability assay showed that while control cells continued to grow, cells in the presence of chelators did not proliferate (Supplemental Fig. 2A). Analysis of the long-term cytotoxicity of Bp4aT, Bp4eT and BpT in PBMCs at 0.3 μM showed that Bp4aT was more toxic compared to Bp4eT or BpT (Fig. 4C). These results showed that while iron chelators were not toxic during the 24 h incubation when the anti-viral effect was observed, longer incubation times demonstrated cytotoxicity. Taken together, the results above demonstrated that among the analyzed iron chelators, Bp4eT was the most promising anti-viral agent.

Molecular Pharmacology Fast Forward. Published on October 18, 2010 as DOI: 10.1124/mol.110.069062
This article has not been copyedited and formatted. The final version may differ from this version.

Examination of the effect of chelators on Sp1- and NF-κB-driven transcription.

Sp1 activity is important for HIV-1 basal transcription (Jochmann et al., 2009) and Tat-induced HIV-1 transcription (Chun et al., 1998). NF-κB is activated in various cell types in response to hypoxia and is important for Tat-activated HIV-1 transcription, as it acts in concert with Tat and CDK9/cyclin T1 (West et al., 2001). Considering this, to determine whether iron chelators have an effect on NF-κB- and Sp1-driven activity, we analyzed their effect on the NF-κB-dependent *e-selectin* promoter as a relevant positive control (Fu et al., 2003). This was then compared to the effects of the chelators on the activity of *HIV-1* promoters with the deletion of NF-κB sites or inactivation of Sp1 sites in 293T cells (Gomez-Gonzalo et al., 2001). Bp4eT at 10 μM inhibited the activity of WT HIV-1 LTR in the HIV-1 proviral pNL4-3.Luc.R^-E^- (pNL-Luc) promoter in 293T cells (Fig. 5A). In contrast, the activity of the NF-κB-dependent *e-selectin* promoter (Fu et al., 2003) was not affected in 293T cells incubated with this chelator (Fig. 5A). This suggested that NF-κB activity was not changed after incubation of cells with iron chelators. It should be noted that analysis of cytotoxicity in 293T cells by the calcein-AM uptake assay showed that Bp4eT (10 μM) did not exhibit significant toxicity compared to the control after 24 h (Supplemental Fig. 2B).

In the absence of Tat, basal activity of the WT HIV-1 LTR promoter (denoted WT KB SP) was reduced by 2.7-fold in 293T cells incubated with 10 μM Bp4eT (Fig. 5B). In contrast, the activities of the HIV-1 LTR without NF-κB sites (WT SP) or with inactivated Sp1 sites (WT SP 123) were reduced by only 1.3- and 1.4-fold, respectively (Fig. 5B). These results indicated that inactivation of Sp1 sites or deletion of NF-κB sites

Molecular Pharmacology Fast Forward. Published on October 18, 2010 as DOI: 10.1124/mol.110.069062
This article has not been copyedited and formatted. The final version may differ from this version.

makes the remaining promoter activity less sensitive to Bp4eT. Thus, the effect of the iron chelators on basal HIV-1 transcription might involve de-regulation of a factor other than Sp1 or NF-κB. Other possible factors that could be affected by the chelators include CDK9/cyclin T1 and this is assessed below.

Inhibition of CDK2.

Previously, we demonstrated that 311 and ICL670 inhibited CDK2 activity (Debebe et al., 2007). To determine if the most effective BpT and DpT chelators had a similar effect, CDK2 was immunoprecipitated from 293T cells incubated for 24 h at 37^{o}C with Dp44mT, Bp4aT or Bp4eT and also the positive control chelators, 311 or ICL670 (all at 10 μM except ICL670A that was used at 100 μM due to its low efficacy; Fig. 6A). These studies showed that Bp4eT, Dp44mT and particularly Bp4aT, were significantly (p<0.001) more active than 311 or ICL670 at inhibiting CDK2 kinase activity (Fig. 6A).

Next, we analyzed whether the inhibition of CDK2 activity parallels the inhibition of HIV-1 transcription using 293T cells. CDK2 was immunoprecipitated from 293T cells incubated with three different concentrations of Bp4eT (0.1, 1 and 10 μM) and its activity was analyzed with histone H1 as a substrate. Histone H1 phosphorylation was reduced in a dose-dependent manner with about 50% inhibition at 1 μM and 85% inhibition at 10 μM (Figs. 6B and C), being consistent with the inhibition of HIV-1 transcription (IC_{50} = 2 μM; Fig. 3A).

Molecular Pharmacology Fast Forward. Published on October 18, 2010 as DOI: 10.1124/mol.110.069062
This article has not been copyedited and formatted. The final version may differ from this version.

Inhibition of CDK9.

We then analyzed whether CDK9 activity was affected in 293T cells incubated with iron chelators (all at 10 μM except ICL670A at 100 μM) for 24 h at 37^{o}C. This was important to assess as CDK9/cyclin T1 is recruited by HIV-1 Tat to the *HIV-1* promoter and is crucial for viral replication (Nekhai and Jeang, 2006). Cyclin T1 was immunoprecipitated (Fig. 7A) and the activity of co-precipitated CDK9 was assayed with GST-CTD as a substrate. The hyper-phosphorylated *C*-terminal domain of RNA polymerase II (CTDo) that contains more than 3 phosphorylated serine residues migrates as a higher molecular weight band on SDS-PAGE (Fig. 7A). In contrast, the hypo-phosphorylated *C*-terminal domain of RNA polymerase II (CTDa), which appears as a lower molecular weight band on SDS-PAGE (Fig. 7A), co-migrates with the non-phosphorylated CTD of RNA Polymerase II. CTD phosphorylation by CDK9/cyclin T1 resulted in formation of CTDo (Fig.7A, lane 2). There was a significant (p<0.005) decrease in the CTD kinase activity of CDK9/cyclin T1 in cells incubated with all the chelators (Fig. 7A).

Interestingly, we could not detect CDK9 that co-precipitated with cyclin T1 in cells incubated with most iron chelators, except for Bp4aT and Dp44mT, where only very faint bands were observed (Fig. 7A). Analysis of the kinase activity of CDK9 precipitated with anti-CDK9 antibody showed a marked inhibition of CDK9 activity (as demonstrated by a decrease in the intensity of the CTDo and CTDa bands) in the cells incubated with Bp4eT (10 μM) compared to untreated control cells or cells incubated with the negative control, Dp2mT (10 μM; Fig. 7B).

Molecular Pharmacology Fast Forward. Published on October 18, 2010 as DOI: 10.1124/mol.110.069062
This article has not been copyedited and formatted. The final version may differ from this version.

We then determined whether the effect of CDK9 inhibition could be due to changes in its interaction with cyclin T1 and distribution between small CDK9/cyclin T1 complexes and large CDK9/cyclin T1/HEXIM1/7SK RNA complexes. We analyzed the distribution of CDK9 and cyclin T1 between the small and large complexes using the procedure described by Biglione and colleagues (Biglione et al., 2007). Using this method, large and small complexes are sequentially extracted with low salt (LS) and high salt (HS) concentrations. Levels of CDK9 after incubating 293T cells with Bp4eT (1 μM) for 24 h at 37^{o}C were lower than that of the control in both LS and HS extracts, whereas cyclin T1 levels were reduced only in the HS fraction (Fig. 8A and B). These results indicate that the overall level of CDK9 expression is reduced. Further, the amount of high molecular weight CDK9/cyclin T1 complex, which supplies CDK9/cyclin T1 for HIV-1 transcription (Biglione et al., 2007), was reduced after incubation with Bp4eT as demonstrated by the reduction of CDK9 in this complex (Fig. 8B).

Taken together, our data show that HIV-1 transcription is efficiently inhibited by Bp4eT and Bp4aT-based without apparent cytotoxicity over 24 h. This mechanism of inhibition may include the inhibition of CDK9/cyclin T1 activity, in addition to the previously shown inhibition of CDK2 activity (Debebe et al., 2007).

Molecular Pharmacology Fast Forward. Published on October 18, 2010 as DOI: 10.1124/mol.110.069062
This article has not been copyedited and formatted. The final version may differ from this version.

Discussion

Iron is required for several steps in the HIV-1 life cycle including reverse transcription, HIV-1 gene expression and capsid assembly (Drakesmith and Prentice, 2008). Therefore, the use of Fe chelators as a therapeutic strategy has potential and needs to be carefully assessed. Here, we focused on the effect of iron chelators on HIV-1 transcription and identified Bp4aT and Bp4eT as the two most promising agents that inhibited HIV-1 transcription in cultured cell lines and primary cells. Bp4eT was relatively non-toxic after a 24 h incubation and could be the most suitable candidate as a potential HIV-1 inhibitor. However, only Bp4aT effectively inhibited HIV-1 transcription in primary PMBCs, and thus, should also be further considered.

CDK2, a previously identified regulator of HIV-1 transcription (reviewed in (Nekhai and Jeang, 2006)), was found to be a molecular target of the BpT and DpT chelators. Thus, CDK2 inhibition could partly be responsible for the anti-viral activity of the chelators. Inhibition of CDK2 by either pharmacological inhibitors or by CDK2-directed siRNA has been shown to suppress HIV-1 replication (Agbottah et al., 2005; Ammosova et al., 2005). Iron chelators affect the activity or expression of CDK2 (Debebe et al., 2007; Gao and Richardson, 2001; Pahl et al., 2007) and deregulation of CDK2/cyclin activity by these agents arrests cell cycle progression (Lucas et al., 1995; Pahl et al., 2000). The iron chelator, desferri-exochelin, inhibits the binding of cyclin A and cyclin E to CDK2 in human mammary epithelial cells, whereas in human breast cancer cells the binding is increased (Pahl et al., 2007). On the other hand, the ligand 311 inhibits the expression of cyclins D1, D2, D3, A and B1 and also CDK2, but not cyclin E (Gao and Richardson,

2001). The chelator-mediated mechanism of inhibition of CDK2 activity may include de-regulation of CDK2 binding to cyclin E or cyclin A and also increased binding of the CDK inhibitor, p21, to the CDK2/cyclin A complex. Considering this, iron chelators have been shown to down-regulate p21 protein expression in some cell types (Fu and Richardson, 2007), but up-regulate it in others, the effect being dependent on the cell-type assessed (R. Moussa and D.R. Richardson, unpublished data). Hence, further studies are required to assess the role of p21 in the mechanism of CDK2 inhibition by iron chelators.

In the current study, we demonstrated that the BpT and DpT-based iron chelators can inhibit CDK2 activity. Interestingly, this investigation showed that in addition to the inhibition of CDK2, the chelators also inhibit CDK9/cyclin T1 activity, that is recruited by HIV-1 Tat-induced HIV-1 transcription (Nekhai and Jeang, 2006). CDK9/cyclin T1 is present in cells within a large complex that contains 7SK RNA and the hexamethylene bisacetamide (HEXIM1)-induced protein and also a small complex (reviewed in (Michels and Bensaude, 2008)). The activity of CDK9 in the large complex is inhibited by the interaction with 7SK RNA and HEXIM1. The CDK9 inhibitors, flavopiridol and roscovitin, reduce the formation of the large complex at a concentration that inhibited HIV-1 (Biglione et al., 2007). This suggests that the large complex is important for the activation of HIV-1 transcription and may supply CDK9/cyclin T1 for Tat recruitment. We demonstrate here that CDK9/cyclin T1-kinase activity is markedly inhibited in cells incubated with Bp4aT, Bp4eT or Dp44mT, thus providing a mechanistic explanation for the inhibitory effects of these agents on HIV-1 replication. Our analysis of the large and

Molecular Pharmacology Fast Forward. Published on October 18, 2010 as DOI: 10.1124/mol.110.069062
This article has not been copyedited and formatted. The final version may differ from this version.

small complexes in the cells incubated with iron chelators showed a reduction of the CDK9, but not cyclin T1, in the high molecular weight CDK9/cyclin T1 complex. Hence, the molecular mechanism involved in preventing HIV1 transcription by chelators could involve their targeting and inhibition of CDK9/cyclin T1 activity in addition to CDK2 activity.

HIV-1 basal transcription is largely regulated by the Sp1 transcription factor (Jochmann et al., 2009), while in Tat-activated transcription, NF-κB plays an important regulatory role by acting in concert with Tat and CDK9/cycin T1 (West et al., 2001). Our analysis showed that transcription from the NF-κB-dependent *e-selectin* promoter was not changed in cells incubated with Bp4eT, thus excluding NF-κB as a target for iron chelators. However, because inactivation of Sp1 as well as NF-κB sites equally decreased sensitivity of the *HIV-1* promoter to iron chelator treatment, it is possible that these agents cooperatively affect both the NF-κB and Sp1 sites. Since NF-κB acts in concert with CDK9/cyclin T1 (West et al., 2001) and Sp1 targets CDK9/cyclin T1 to the *HIV-1* promoter in the absence of Tat (Yedavalli et al., 2003), the inactivation of CDK9/cyclin T1 might affect both NF-κB and Sp1-driven transcription of the *HIV-1* promoter.

Considering the potential mechanism of the anti-HIV activity of the chelators and the possible role of CDK2 as their molecular target, it is significant to consider the following studies. CDK2 knock-out mice are viable, although CDK2 is required for germ cell development, since CDK2 (-/-) mice are sterile (Berthet et al., 2003). In the absence of CDK2, CDK1 compensates for its loss (Satyanarayana et al., 2008). However, the

impairment of DNA repair activity makes CDK2 (-/-) mice more sensitive to lethal irradiation (Satyanarayana et al., 2008). Interestingly, while CDK2 activity is needed for proliferation of cultured lymphocytes, proliferation of human marrow cells is driven by CDK1 combined with either cyclin A or cyclin B (Xie et al., 2008). Thus, CDK2 may be dispensable for proliferation and survival of some cells *in vivo*, and if so, inhibitors of CDK2 might be considered as a novel class of anti-HIV-1 therapeutics.

In addition to the inhibition of HIV-1 transcription, iron-depletion may affect other steps in HIV-1 replication. During viral entry, HIV-1 replication is dependent on the activity of host cell ribonucleotide reductase that contains non-heme iron which is important for enzymatic activity (Tsimberidou et al., 2002). Export of unspliced *HIV-1* mRNA requires HIV-1 Rev protein and host elongation factor 5A (eIF5α). The eIF5α protein contains *N*-epsilon-4-amino-2-hydroxybutyl-lysine (hypusine) that is produced by deoxyhypusine hydroxylase (DOHH), an iron-containing enzyme (Kim et al., 2006). The topical fungicide, cyclopirox (that also is an iron chelator), and the orally-active chelator, deferiprone, inhibit HIV-1 gene expression interfering with the hydroxylation step in the hypusine modification of eIF5α (Hoque et al., 2009). Furthermore, assembly of the HIV capsid requires an ATP-binding protein, ABCE1, which contains iron-sulfur clusters (Barthelme et al., 2007) and binds to HIV-1 Gag protein (Zimmerman et al., 2002). Thus, iron chelators may have a wider spectrum of molecular targets and further studies are required to analyze these.

To assess their possible utility as pharmaceuticals against HIV-1, we compared the anti-viral activity of the most efficient chelators, Bp4aT and Bp4eT, with the previously reported HIV-1 inhibitors, ARC and roscovitin (Agbottah et al., 2005; Nekhai et al., 2007). These studies showed that the ligands were approximately 4-10-fold less efficient inhibitors than ARC (Fig. 3), but very similar to roscovitin. However, the fact that these chelators were not specifically designed for the treatment of HIV-1 demonstrates their clear potential. Further chemical optimization of the design of these ligands for the purpose of inhibition of HIV-1 is vital. Clearly, the good therapeutic index in short-term infectivity assays shown in the current studies must be followed with extensive *in vivo* assessment to ensure high tolerability that is critical for human use (Biglione et al., 2007). Finally, it must be noted that the very different mechanism of action of these chelators compared to other established anti-viral therapies is an advantage of these agents. Hence, they may be useful in terms of treating resistance to AZT and other commercially available anti-viral drugs that is a major emerging problem.

Significantly, previous *in vivo* studies in mice examining the effects of Dp44mT have shown that it does not lead to decreased levels of tissue iron nor could it induce alterations in multiple hematological parameters (Whitnall et al., 2006; Yuan et al., 2004). This finding is probably due to the very low doses of the agents (0.4-0.7 mg/kg) required for efficacy. Moreover, Dp44mT was well tolerated at optimal doses, demonstrating its potential for clinical use (Whitnall et al., 2006; Yuan et al., 2004). Given the levels of cytotoxicity observed after three days *in vitro* in the current studies, questions could arise as to the feasibility of the development of these compounds as anti-

virals. However, many common chemotherapeutic drugs currently in clinical use (*e.g.*, doxorubicin) display marked cytotoxicity profiles *in vitro* (Yuan et al., 2004), but are tolerated at appropriate doses *in vivo* and have led to vast improvements in a variety of disease states. Hence, clearly, the effect *in vitro* is difficult to directly translate to the *in vivo* situation, and as observed with many other drugs, appropriate dosing is key to optimizing anti-viral activity and minimizing toxicity *in vivo.*

In conclusion, these iron chelators represent agents with a therapeutic window and novel mechanism of action that deserves further investigation in terms of their use in future anti-HIV-1 therapeutic regimens. Their potential may be particularly significant where resistance to standard anti-viral therapy occurs.

Acknowledgments

The authors acknowledge Dr. Anna Suter (Novartis, Pharma AG, Ltd., Basel) for ICL670. We appreciate the assistance of Keon Combi, Xiomei Niu and Dillon Robinson for the help in cell counting and toxicity assays. We are also thankful to Dr. Kuan-Teh Jeang (NIAID, NIH) for critical reading and comments on the manuscript. Finally, Dr. Katie Dixon, Ms Zaklina Kovacevic and Dr. Helena Mangs (Iron Metabolism and Chelation Program, University of Sydney) are acknowledged for their thorough assessment of the manuscript.

Molecular Pharmacology Fast Forward. Published on October 18, 2010 as DOI: 10.1124/mol.110.069062
This article has not been copyedited and formatted. The final version may differ from this version.

Authorship Contributions.

Participated in research design: Debebe, Z., Ammosova, T., Breuer, D., Jerebtsova, M., Kashanchi, F., Nekhai, S.

Conducted experiments: Debebe, Z., Ammosova, T., Breuer, D., Kashanchi, F., Nekhai, S.

Contributed new reagents or analytic tools: Lovejoy, D.B., Kalinowski, D.S., Jerebtsova, M., Ray, P., Richardson, D.R.

Performed data analysis: Debebe, Z., Ammosova, T., Breuer, D., Nekhai, S.

Wrote or contributed to the writing of the manuscript: Debebe, Z., Gordeuk, V., Kalinowski, D.S., Lovejoy, D.B., Richardson, D.R., Nekhai, S.

Other: Debebe, Z., Gordeuk, V., Kalinowski, D., Lovejoy, D.B., Richardson, D.R. and Nekhai, S. acquired funding for the research.

References

Agbottah E, de La Fuente C, Nekhai S, Barnett A, Gianella-Borradori A, Pumfery A and Kashanchi F (2005) Antiviral activity of CYC202 in HIV-1-infected cells. *J Biol Chem* **280**(4):3029-3042.

Ammosova T, Berro R, Kashanchi F and Nekhai S (2005) RNA interference directed to CDK2 inhibits HIV-1 transcription. *Virology* **341**(2):171-178.

Barthelme D, Scheele U, Dinkelaker S, Janoschka A, Macmillan F, Albers SV, Driessen AJ, Stagni MS, Bill E, Meyer-Klaucke W, Schunemann V and Tampe R (2007) Structural organization of essential iron-sulfur clusters in the evolutionarily highly conserved ATP-binding cassette protein ABCE1. *J Biol Chem* **282**(19):14598-14607.

Becker EM, Lovejoy DB, Greer JM, Watts R and Richardson DR (2003) Identification of the di-pyridyl ketone isonicotinoyl hydrazone (PKIH) analogues as potent iron chelators and anti-tumour agents. *Br J Pharmacol* **138**(5):819-830.

Berthet C, Aleem E, Coppola V, Tessarollo L and Kaldis P (2003) Cdk2 knockout mice are viable. *Curr Biol* **13**(20):1775-1785.

Biglione S, Byers SA, Price JP, Nguyen VT, Bensaude O, Price DH and Maury W (2007) Inhibition of HIV-1 replication by P-TEFb inhibitors DRB, seliciclib and flavopiridol correlates with release of free P-TEFb from the large, inactive form of the complex. *Retrovirology* **4**:47.

Butera ST, Roberts BD, Lam L, Hodge T and Folks TM (1994) Human immunodeficiency virus type 1 RNA expression by four chronically infected cell lines indicates multiple mechanisms of latency. *J Virol* **68**(4):2726-2730.

Chun RF, Semmes OJ, Neuveut C and Jeang KT (1998) Modulation of Sp1 phosphorylation by human immunodeficiency virus type 1 Tat. *J Virol* **72**(4):2615-2629.

Debebe Z, Ammosova T, Jerebtsova M, Kurantsin-Mills J, Niu X, Charles S, Richardson DR, Ray PE, Gordeuk VR and Nekhai S (2007) Iron chelators ICL670 and 311 inhibit HIV-1 transcription. *Virology* **367**(2):324-333.

Drakesmith H and Prentice A (2008) Viral infection and iron metabolism. *Nat Rev Microbiol* **6**(7):541-552.

Fu D and Richardson DR (2007) Iron chelation and regulation of the cell cycle: 2 mechanisms of posttranscriptional regulation of the universal cyclin-dependent kinase inhibitor p21CIP1/WAF1 by iron depletion. *Blood* **110**(2):752-761.

Fu DX, Kuo YL, Liu BY, Jeang KT and Giam CZ (2003) Human T-lymphotropic virus type I tax activates I-kappa B kinase by inhibiting I-kappa B kinase-associated serine/threonine protein phosphatase 2A. *J Biol Chem* **278**(3):1487-1493.

Gao J and Richardson DR (2001) The potential of iron chelators of the pyridoxal isonicotinoyl hydrazone class as effective antiproliferative agents, IV: The mechanisms involved in inhibiting cell-cycle progression. *Blood* **98**(3):842-850.

Georgiou NA, van der Bruggen T, Oudshoorn M, Hider RC, Marx JJ and van Asbeck BS (2002) Human immunodeficiency virus type 1 replication inhibition by the bidentate iron chelators CP502 and CP511 is caused by proliferation inhibition and the onset of apoptosis. *Eur J Clin Invest* **32** Suppl 1:91-96.

Georgiou NA, van der Bruggen T, Oudshoorn M, Nottet HS, Marx JJ and van Asbeck BS (2000) Inhibition of human immunodeficiency virus type 1 replication in human

mononuclear blood cells by the iron chelators deferoxamine, deferiprone, and bleomycin. *J Infect Dis* **181**(2):484-490.

Gomez-Gonzalo M, Carretero M, Rullas J, Lara-Pezzi E, Aramburu J, Berkhout B, Alcami J and Lopez-Cabrera M (2001) The hepatitis B virus X protein induces HIV-1 replication and transcription in synergy with T-cell activation signals: functional roles of NF-kappaB/NF-AT and SP1-binding sites in the HIV-1 long terminal repeat promoter. *J Biol Chem* **276**(38):35435-35443.

Gordeuk VR, Delanghe JR, Langlois MR and Boelaert JR (2001) Iron status and the outcome of HIV infection: an overview. *J Clin Virol* **20**(3):111-115.

He J and Landau NR (1995) Use of a novel human immunodeficiency virus type 1 reporter virus expressing human placental alkaline phosphatase to detect an alternative viral receptor. *J Virol* **69**(7):4587-4592.

Hershko C (1994) Control of disease by selective iron depletion: a novel therapeutic strategy utilizing iron chelators. *Baillieres Clin Haematol* **7**(4):965-1000.

Hoque M, Hanauske-Abel HM, Palumbo P, Saxena D, D'Alliessi Gandolfi D, Park MH, Pe'ery T and Mathews MB (2009) Inhibition of HIV-1 gene expression by Ciclopirox and Deferiprone, drugs that prevent hypusination of eukaryotic initiation factor 5A. *Retrovirology* **6**:90.

Jochmann R, Thurau M, Jung S, Hofmann C, Naschberger E, Kremmer E, Harrer T, Miller M, Schaft N and Sturzl M (2009) O-linked N-acetylglucosaminylation of Sp1 inhibits the human immunodeficiency virus type 1 promoter. *J Virol* **83**(8):3704-3718.

Kalinowski DS, Yu Y, Sharpe PC, Islam M, Liao YT, Lovejoy DB, Kumar N, Bernhardt PV and Richardson DR (2007) Design, synthesis, and characterization of novel iron chelators: structure-activity relationships of the 2-benzoylpyridine thiosemicarbazone series and their 3-nitrobenzoyl analogues as potent antitumor agents. *J Med Chem* **50**(15):3716-3729.

Kim YS, Kang KR, Wolff EC, Bell JK, McPhie P and Park MH (2006) Deoxyhypusine hydroxylase is a Fe(II)-dependent, HEAT-repeat enzyme. Identification of amino acid residues critical for Fe(II) binding and catalysis [corrected]. *J Biol Chem* **281**(19):13217-13225.

Lucas JJ, Szepesi A, Domenico J, Takase K, Tordai A, Terada N and Gelfand EW (1995) Effects of iron-depletion on cell cycle progression in normal human T lymphocytes: selective inhibition of the appearance of the cyclin A-associated component of the p33cdk2 kinase. *Blood* **86**(6):2268-2280.

Michels AA and Bensaude O (2008) RNA-driven cyclin-dependent kinase regulation: when CDK9/cyclin T subunits of P-TEFb meet their ribonucleoprotein partners. *Biotechnol J* **3**(8):1022-1032.

Nekhai S, Bhat UG, Ammosova T, Radhakrishnan SK, Jerebtsova M, Niu X, Foster A, Layden TJ and Gartel AL (2007) A novel anticancer agent ARC antagonizes HIV-1 and HCV. *Oncogene* **26**(26):3899-3903.

Nekhai S and Jeang KT (2006) Transcriptional and post-transcriptional regulation of HIV-1 gene expression: role of cellular factors for Tat and Rev. *Future Microbiol* **1**:417-426.

Pahl PM, Reese SM and Horwitz LD (2007) A lipid-soluble iron chelator alters cell cycle regulatory protein binding in breast cancer cells compared to normal breast cells. *J Exp Ther Oncol* **6**(3):193-200.

Pahl PM, Yan XD, Hodges YK, Rosenthal EA, Horwitz MA and Horwitz LD (2000) An exochelin of Mycobacterium tuberculosis reversibly arrests growth of human vascular smooth muscle cells in vitro. *J Biol Chem* **275**(23):17821-17826.

Papadopoulos NG, Dedoussis GV, Spanakos G, Gritzapis AD, Baxevanis CN and Papamichail M (1994) An improved fluorescence assay for the determination of lymphocyte-mediated cytotoxicity using flow cytometry. *J Immunol Methods* **177**(1-2):101-111.

Porter JB (2006) Deferasirox: An effective once-daily orally active iron chelator. *Drugs Today (Barc)* **42**(10):623-637.

Satyanarayana A, Hilton MB and Kaldis P (2008) p21 Inhibits Cdk1 in the absence of Cdk2 to maintain the G1/S phase DNA damage checkpoint. *Mol Biol Cell* **19**(1):65-77.

Traore HN and Meyer D (2004) The effect of iron overload on in vitro HIV-1 infection. *J Clin Virol* **31 Suppl 1**:S92-98.

Tsimberidou AM, Alvarado Y and Giles FJ (2002) Evolving role of ribonucleoside reductase inhibitors in hematologic malignancies. *Expert Rev Anticancer Ther* **2**(4):437-448.

West MJ, Lowe AD and Karn J (2001) Activation of human immunodeficiency virus transcription in T cells revisited: NF-kappaB p65 stimulates transcriptional elongation. *J Virol* **75**(18):8524-8537.

Whitnall M, Howard J, Ponka P and Richardson DR (2006) A class of iron chelators with a wide spectrum of potent antitumor activity that overcomes resistance to chemotherapeutics. *Proc Natl Acad Sci U S A* **103**(40):14901-14906.

Xie DX, Yao J, Zhang P, Li XL, Feng YD, Wu JH, Tao DD, Hu JB and Gong JP (2008) Are progenitor cells pre-programmed for sequential cell cycles not requiring cyclins D and E and activation of Cdk2? *Cell Prolif* **41**(2):265-278.

Yedavalli VS, Benkirane M and Jeang KT (2003) Tat and trans-activation-responsive (TAR) RNA-independent induction of HIV-1 long terminal repeat by human and murine cyclin T1 requires Sp1. *J Biol Chem* **278**(8):6404-6410.

Yuan J, Lovejoy DB and Richardson DR (2004) Novel di-2-pyridyl-derived iron chelators with marked and selective antitumor activity: in vitro and in vivo assessment. *Blood* **104**(5):1450-1458.

Zimmerman C, Klein KC, Kiser PK, Singh AR, Firestein BL, Riba SC and Lingappa JR (2002) Identification of a host protein essential for assembly of immature HIV-1 capsids. *Nature* **415**(6867):88-92.

Molecular Pharmacology Fast Forward. Published on October 18, 2010 as DOI: 10.1124/mol.110.069062
This article has not been copyedited and formatted. The final version may differ from this version.

Footnotes

a) This project was supported by National Institutes of Health grants from the National Heart, Lung, and Blood Institute and The Office of Research on Minority Health [2R25 HL003679-08; RO1 HL55605 and F31 HL090025]; National Center for Research Resources [2MO1 RR10284]; National Institute of General Medicine [1SC1GM082325]; Research Centers in Minority Institutions (RCMI) Program of the Division of Research Infrastructure, National Center for Research Resources [RCMI-NIH 2G12RR003048]; The National Institute of Diabetes and Digestive and Kidney Diseases **[**RO1 DK49419]; National Center for Complimentary and Alternative Medicine [R21 AT002278]; and by a Senior Principal Research Fellowship [#571123] and a Project Grant [#570952] from the National Health and Medical Research Council of Australia.

b) Des R. Richardson, Iron Metabolism and Chelation Program, Department of Pathology and Bosch Institute, Blackburn Building (D06), University of Sydney, Sydney, New South Wales, 2006 Australia; Telephone: +61-2-9036-6548; Fax: +61-2-9351-3429 ; E-mail: d.richardson@med.usyd.edu.au

c) [1]The senior authors of this article that contributed equally.

Molecular Pharmacology Fast Forward. Published on October 18, 2010 as DOI: 10.1124/mol.110.069062
This article has not been copyedited and formatted. The final version may differ from this version.

Legends for Figures

Figure 1. Structures of the chelators used in this study (A) and the effect of DpT- and BpT-based iron chelators on HIV-1 transcription (B and C) in CEM GFP cells. **(A)** Chemical structures of the iron chelators examined in this study including members of the di-2-pyridylketone thiosemicarbazone (DpT) series, 2-benzoylpyridine thiosemicarbazone (BpT) series, 2-(3-nitrobenzoyl)pyridine thiosemicarbazone (NBpT) series, di-2-pyridylketone thiobenzoyl hydrazone (PKTBH) and 2-benzoylpyridine thiobenzoyl hydrazone (BPTBH). **(B & C) Inhibition of HIV-1 transcription in CEM-GFP cells**. CEM-GFP cells were infected with Adeno-Tat and then incubated with the indicated chelators for 24 h at 37^{o}C. GFP fluorescence was measured in live cells. Figures 1B and 1C show different iron chelators that were separated into 2 graphs for clarity. The chelators enclosed in boxes were those with the lowest IC_{50} values for inhibition of HIV-1 transcription. IC_{50} values were determined using GraphPad Prism 3 software as described in the *Materials and Methods.* Results are means of 3 independent experiments.

Figure 2. Effect of chelators on HIV-1 replication. (A) Effect of chelators on one round of HIV-1-Luc replication in CEM T cells. CEM T cells were infected with VSVG-pseudotyped pNL4-3.Luc.R-E- (HIV-1 Luc) virus for 18 h at 37^{o}C and then incubated for 24 h at 37^{o}C with the indicated concentrations of iron chelators as shown in the figure. Luciferase activity was then measured and values presented as mean ± SD (n = 4) in a typical experiment of 3 independent experiments performed. IC_{50} values were determined using GraphPad Prism 3 software. **(B) Anti-HIV-1 activity of Bp4aT and Bp4eT in PBMCs infected with pseudotype HIV-1-Luc.** PBMCs were infected with

Molecular Pharmacology Fast Forward. Published on October 18, 2010 as DOI: 10.1124/mol.110.069062
This article has not been copyedited and formatted. The final version may differ from this version.

VSVG-pseudotyped HIV-1 Luc virus. After 48 h at 37°C, cells were seeded on 96 well plates and incubated with the chelators at the indicated concentrations for 24 h at 37°C. Later, luciferase buffer was added to each well and luciferase activity was measured. IC_{50} values were determined using GraphPad Prism 3 software. **(C) Inhibition of HIV-1 replication in OM10.1 cells by Bp4aT and Bp4eT.** HIV-1 replication was induced in OM10.1 cells as described in the *Materials and Methods* and the cells were subsequently treated with the indicated concentrations of Bp4aT or Bp4eT for 48 h at 37°C. Media was collected and the activity of reverse transcriptase determined as described in the *Materials and Methods*. Values presented are mean ± SD (n = 3) in a typical experiment of 3 performed.

Figure 3. Inhibition of Tat-induced HIV-1 transcription using 293T cells by iron chelators, and CDK9 and CDK2 inhibitors, ARC and roscovitin. 293T cells were transfected with HIV-1 LTR-Lac Z, CMV-EGFP and Tat-expression vectors and then incubated with the indicated concentrations of iron chelators **(A)** or the CDK9 and CDK2 inhibitors, ARC or Roscovitin **(B)** for 24 h at 37°C. HIV-1 transcription was analyzed by measuring β-galactosidase activity. The results are mean ± SD (n = 4) and are typical of 3 independent experiments. The IC_{50} values were calculated using GraphPad Prism 3 software.

Figure 4. Effect of iron chelators on viability of CEM T cells and PBMCs. (A) Short-term effect of Bp4aT and Bp4eT on the viability of CEM T cells. CEM T cells were incubated with the indicated concentrations of the chelators for 24 h at 37°C. The cells were then washed with PBS, incubated with 0.2 μM calcein-AM for 15 min at 37°C and

Molecular Pharmacology Fast Forward. Published on October 18, 2010 as DOI: 10.1124/mol.110.069062
This article has not been copyedited and formatted. The final version may differ from this version.

fluorescence was measured at an excitation of 495 nm and an emission of 515 nm. Values presented are mean ± SD (*n* = 4) and are typical of 3 independent experiments. **(B) Long-term effect of Bp4aT and Bp4eT on the viability of CEM T cells.** CEM T cells were incubated with Bp4aT, Bp4eT, and BpT at 10 μM for 24, 48, 72, 96 and 120 h at 37^{o}C. The cells were then washed with PBS, incubated with 0.2 μM calcein-AM for 15 min at 37^{o}C and fluorescence was measured at an excitation of 495 nm and an emission of 515 nm. Values presented are mean ± SD (*n* = 4) and are typical of 3 independent experiments. **(C) Long-term effect of Bp4aT and Bp4eT on the viability of PBMC.** PBMC cells were incubated with the iron chelators (0.3 μM) for the indicated number of days at 37^{o}C. Cells were then washed with PBS, incubated with 0.2 μM calcein-AM for 15 min at 37^{o}C and fluorescence was measured at an excitation of 495 nm and an emission of 515 nm. Values presented are mean ± SD (*n* = 4) and are typical of 3 independent experiments.

Figure 5. Effect of Bp4eT on transcription from HIV-1 and e-selectin promoters. (A) Effect of iron chelators on *HIV-1* and *e-selectin* promoters. 293T cells were transiently transfected with the CMV-EGFP reporter in combination with e-selectin-luciferase (a NF-κB driven promoter), or pNL4-3.Luc.R^{-}E^{-} (*HIV-1* promoter). The cells were incubated for 24 h at 37^{o}C in the absence or presence of Bp4eT (10 μM). The cells were lysed and the luciferase activity was measured. In parallel, EGFP fluorescence was measured and used for normalization. Values presented are mean ± SD (*n* = 4) in a typical experiment of two independent experiments performed. **(B) Effect of iron chelators on basal transcription of HIV-1 LTR with deletion of NF-κB sequences and**

Molecular Pharmacology Fast Forward. Published on October 18, 2010 as DOI: 10.1124/mol.110.069062
This article has not been copyedited and formatted. The final version may differ from this version.

inactivation of Sp1 sites. 293T cells were transiently transfected with WT HIV-1 LTR (-105 to +77)-*luciferase* reporter (WT SP KB), HIV-1 LTR (-81 to +77) with NF-κB-deleted sites (WT SP) or HIV-1 LTR (-105 to +77) with Sp1 inactivated sites (WT SP 123). The cells were also co-transfected with the CMV-GFP expression vector. The cells were incubated with Bp4eT (10 μM) for 18 h at 37^{o}C, then lysed and luciferase activity measured. In parallel, EGFP fluorescence was measured and used for normalization. Values presented are mean ± SD (n = 4) in a typical experiment of two independent experiments performed.

Figure 6. Effect of iron chelators on CDK2 activity. (A) Inhibition of CDK2 activity by chelators. 293T cells were incubated with 311 (10 μM), ICL670 (100 μM) or Bp4aT (10 μM), Bp4eT (10 μM) or Dp44mT (10 μM) for 24 h at 37^{o}C. The cells were lysed and CDK2 was immunoprecipitated as described in *Materials and Methods*. **Top panel**: The precipitated CDK2 was resolved on 10% SDS-PAGE and immunoblotted with antibody against CDK2. **Bottom panel:** Immunoprecipitated CDK2 was used for the *in vitro* kinase assay using histone H1 as substrate. Phosphorylated histone H1 was resolved on SDS-PAGE and detected on a Phosphor imager. Results presented are typical gels from 3 independent experiments. **(B) Dose-dependent inhibition of CDK2 activity with Bp4eT**. 293T cells were incubated with Bp4eT at concentrations of 0.1, 1.0, and 10 μM for 24 h at 37^{o}C. **Top panel:** The level of tubulin, as a loading control, was resolved using SDS-PAGE and detected by immunoblotting. **Middle panel**: CDK2 was immunoprecipitated as described in *Materials and Methods*. The precipitated CDK2 was resolved on 10% SDS-PAGE and immunoblotted with antibody against CDK2. **Bottom**

Molecular Pharmacology Fast Forward. Published on October 18, 2010 as DOI: 10.1124/mol.110.069062
This article has not been copyedited and formatted. The final version may differ from this version.

panel: CDK2 was precipitated as above and immunoprecipitated CDK2 was subsequently incubated with histone H1 in the presence of γ-(^{32}P) ATP. Kinase reactions were resolved on 10% SDS-PAGE and analyzed on a Phosphor Imager. **(C)** The density of the bands from the kinase reaction in the bottom panel B was quantified and presented in arbitrary units.

Figure 7. Effect of iron chelators on CDK9 activity. (A) Inhibition of CDK9 activity. 293T cells were incubated with iron chelators (all at 10 μM except ICL670A at 100 μM) for 24 h at 37^{o}C. The cells were lysed and CDK9/cyclin T1 was immunoprecipitated using anti-cyclin T1 antibody. The precipitated proteins were resolved on 10% SDS-PAGE and immunoblotted with antibody against cyclin T1 (**Top panel**) and CDK9 (**middle panel**) respectively. **Bottom panel,** immunoprecipitated cyclin T1 was used for the *in vitro* kinase assay using GST-CTD as the substrate. Phosphorylated GST-CTD was resolved by SDS-PAGE and detected using a Phosphor imager. Positions of hyper- and hypo-phosphorylated CTD are indicated as CTDo and CTDa. **(B)** 293T cells were incubated with Bp4eT or Dp2mT (10 μM) for 24 h at 37^{o}C. The cells were then lysed and CDK9 was immunoprecipitated using anti-CDK9 antibody. Immunoprecipitated CDK9 was used for the *in vitro* kinase assay using GST-CTD as the substrate. Phosphorylated GST-CTD was resolved by SDS-PAGE and detected using a Phosphor imager. Positions of hyper- and hypo-phosphorylated CTD are indicated as CTDo and CTDa, respectively. Densitometry represents the intensity of CTDo and is presented as arbitrary units. Results presented are typical gels from 3 independent experiments.

Molecular Pharmacology Fast Forward. Published on October 18, 2010 as DOI: 10.1124/mol.110.069062
This article has not been copyedited and formatted. The final version may differ from this version.

Figure 8. Analysis of CDK9 and cyclin T1 in large and small complexes. 293T cells were incubated with Bp4eT (1 μM) for 24 h at 37^{o}C, and CDK9/cyclin T1-containing large and small complexes were extracted using a low salt (LS) and high salt (HS) buffers respectively, as described in the *Methods and Materials*. **(A)** The lysates were resolved by 10% SDS-PAGE and immunoblotted using antibody against CDK9 and cyclin T1. The panels on the left show large complexes extracted with the LS buffer and the panels on the right show small complexes extracted with the HS buffer. **(B)** The intensity of the bands from **(A)** was quantified and presented in arbitrary units. Results are from a typical experiment of 2 performed.

Molecular Pharmacology Fast Forward. Published on October 18, 2010 as DOI: 10.1124/mol.110.069062
This article has not been copyedited and formatted. The final version may differ from this version.

Table 1. Effect of DpT and BpT-based iron chelators on HIV-1 transcription and cytotoxicity over a 24 h incubation period. IC_{50} values were determined using Graph Pad Prism software. Results are mean values from 3 experiments.

Number	Chelator	Inhibition of HIV-1 transcription in CEM T cells, IC_{50} (μM)	Cytotoxicity CEM T cells, IC_{50} (μM)
1	DpT	>10	>10
2	Dp2mT	> 3	>10
3	Dp44mT	0.144	>10
4	Dp4aT	0.621	>10
5	Dp4pT	0.134	2.1
6	BpT	> 3	>10
7	Bp4mT	0.318	>10
8	Bp44mT	0.015	2
9	Bp4eT	0.058	>10
10	Bp4aT	0.127	>10
11	Bp4pT	0.042	0.9
12	NBp4eT	0.249	>10
13	NBp4aT	0.500	>10
14	PKTBH	0.200	1.2
15	BPTBH	> 10	>10

Molecular Pharmacology Fast Forward. Published on October 18, 2010 as DOI: 10.1124/mol.110.069062
This article has not been copyedited and formatted. The final version may differ from this version.

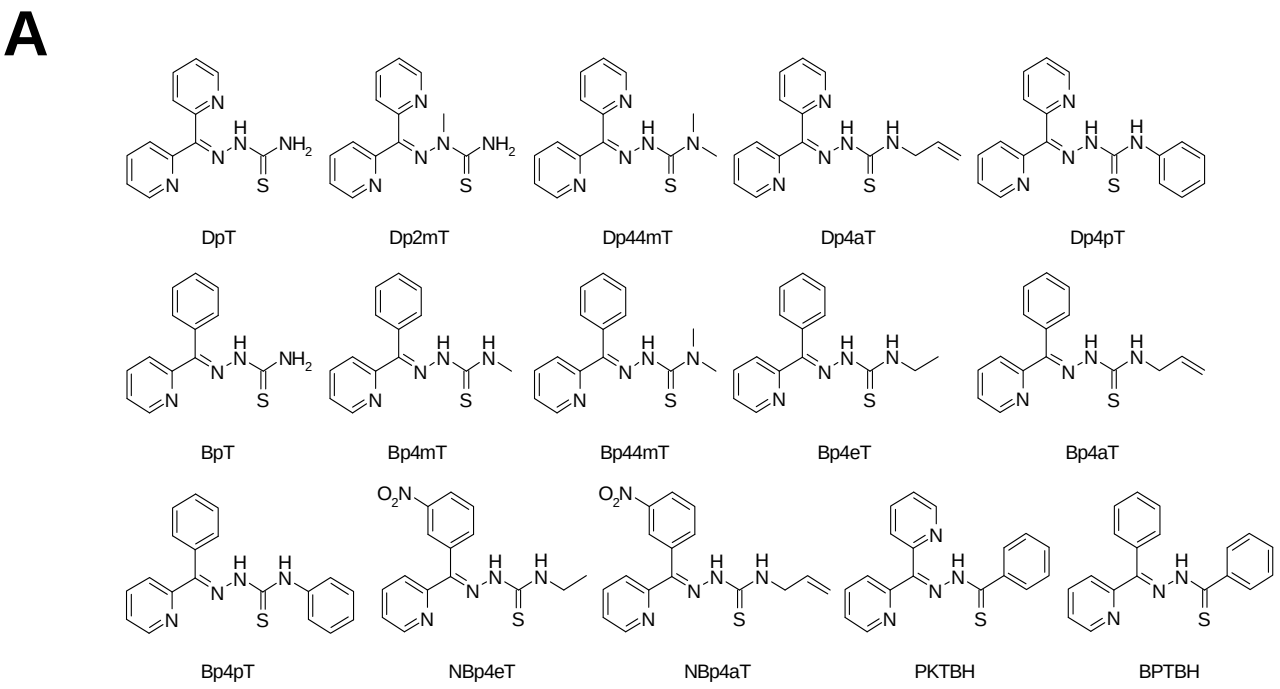

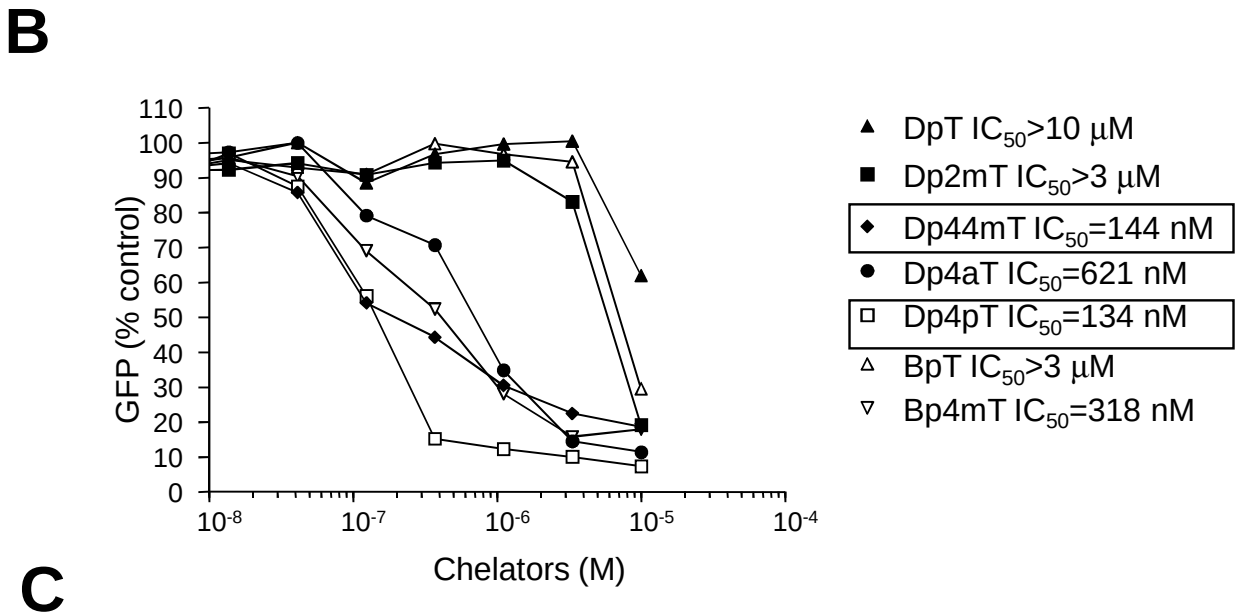

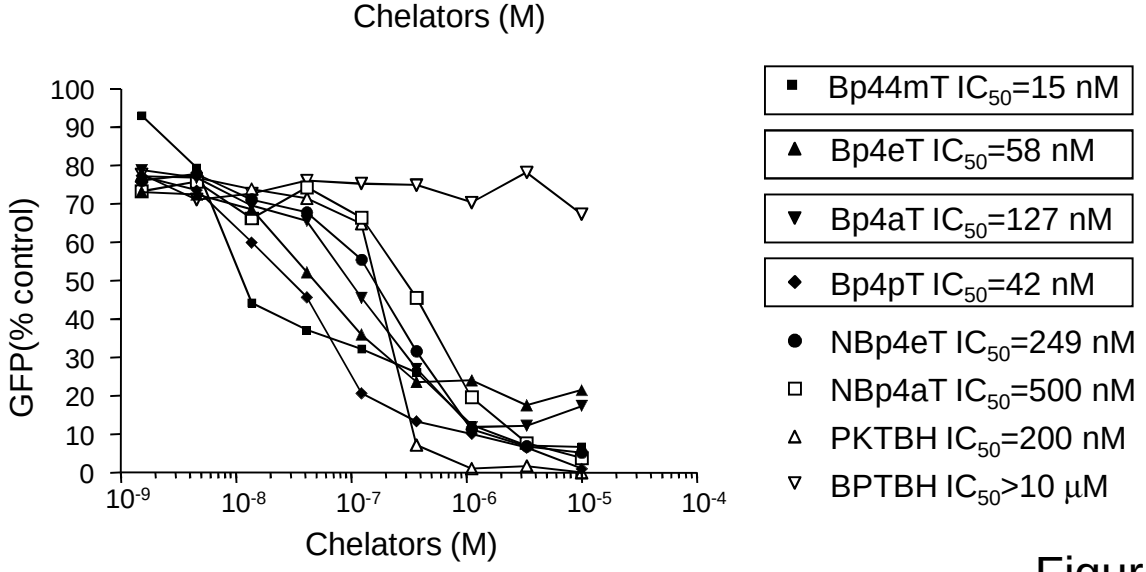

Figure 1

Molecular Pharmacology Fast Forward. Published on October 18, 2010 as DOI: 10.1124/mol.110.069062
This article has not been copyedited and formatted. The final version may differ from this version.

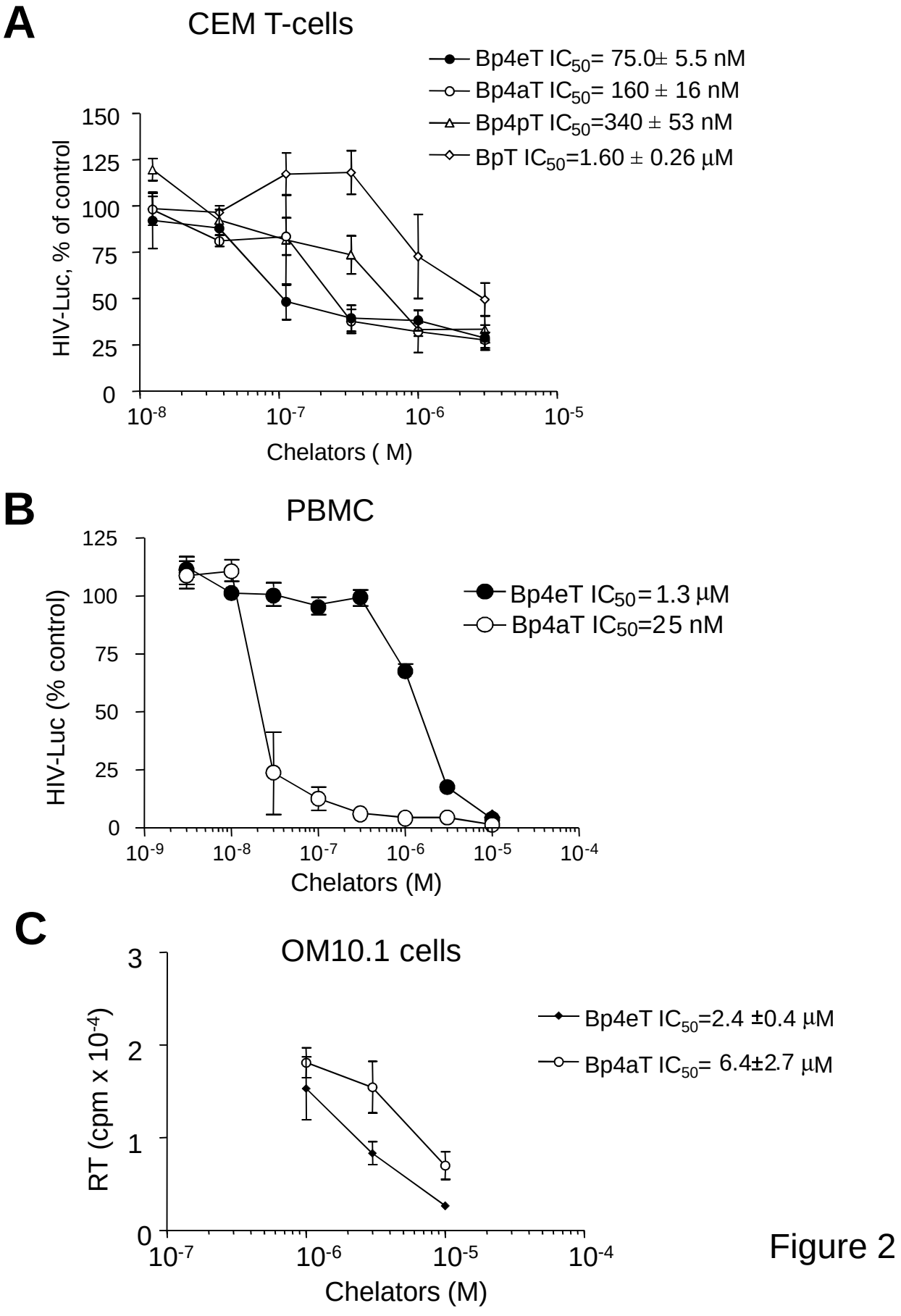

Figure 2

Molecular Pharmacology Fast Forward. Published on October 18, 2010 as DOI: 10.1124/mol.110.069062
This article has not been copyedited and formatted. The final version may differ from this version.

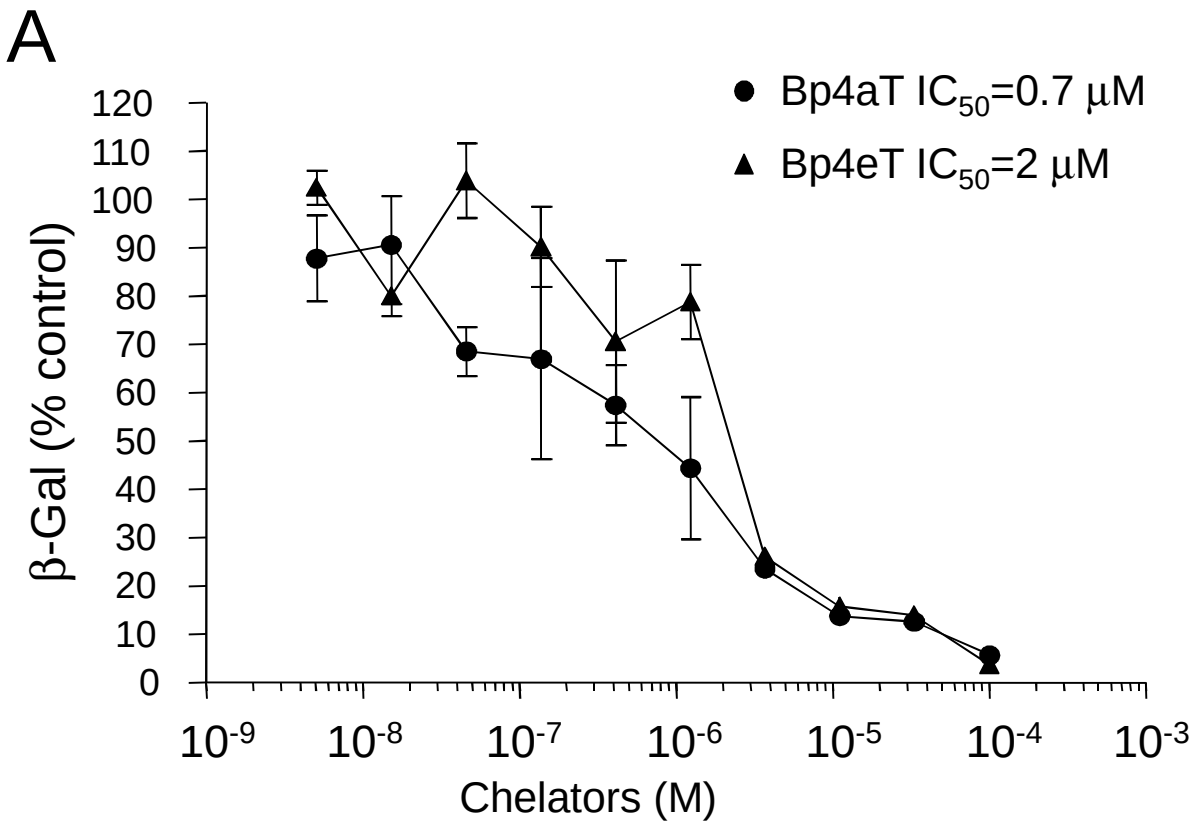

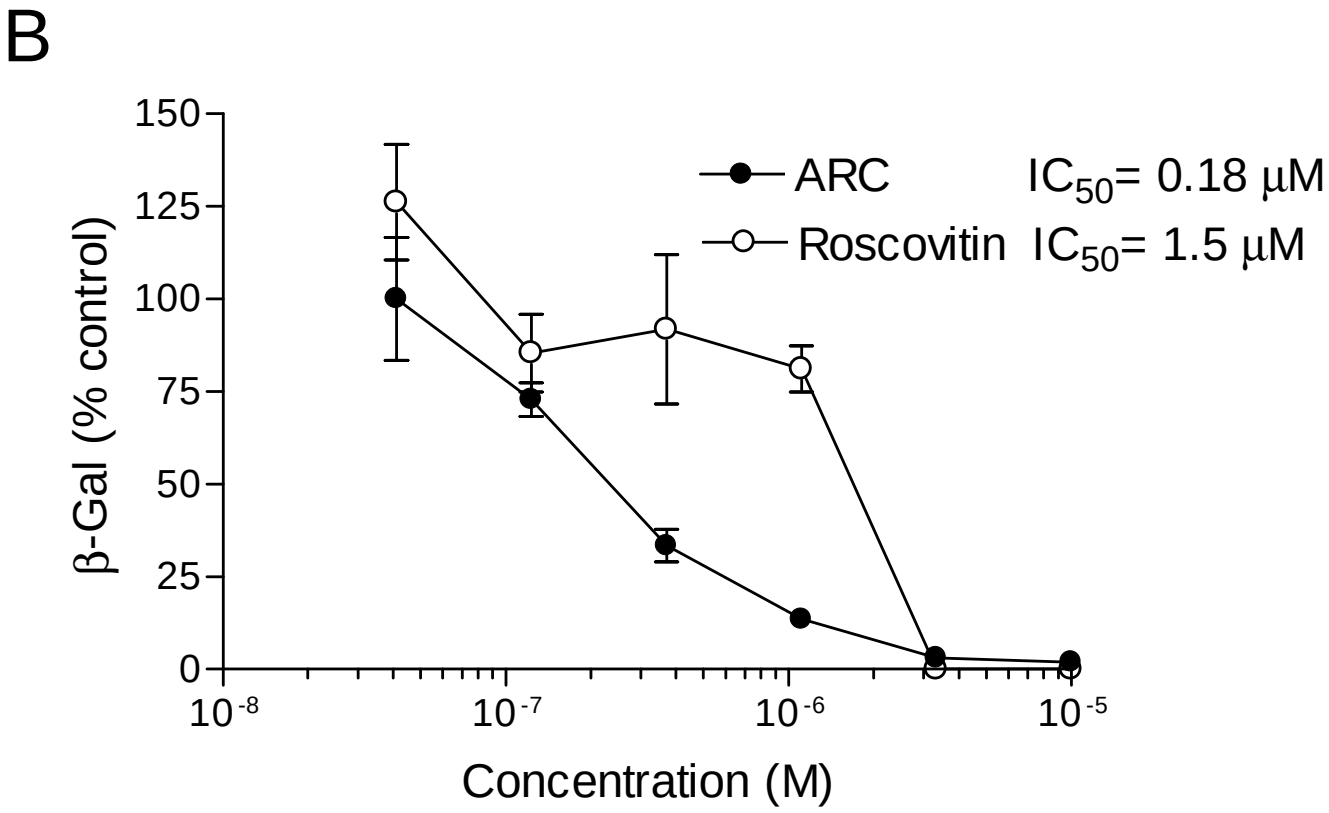

Figure 3

Molecular Pharmacology Fast Forward. Published on October 18, 2010 as DOI: 10.1124/mol.110.069062
This article has not been copyedited and formatted. The final version may differ from this version.

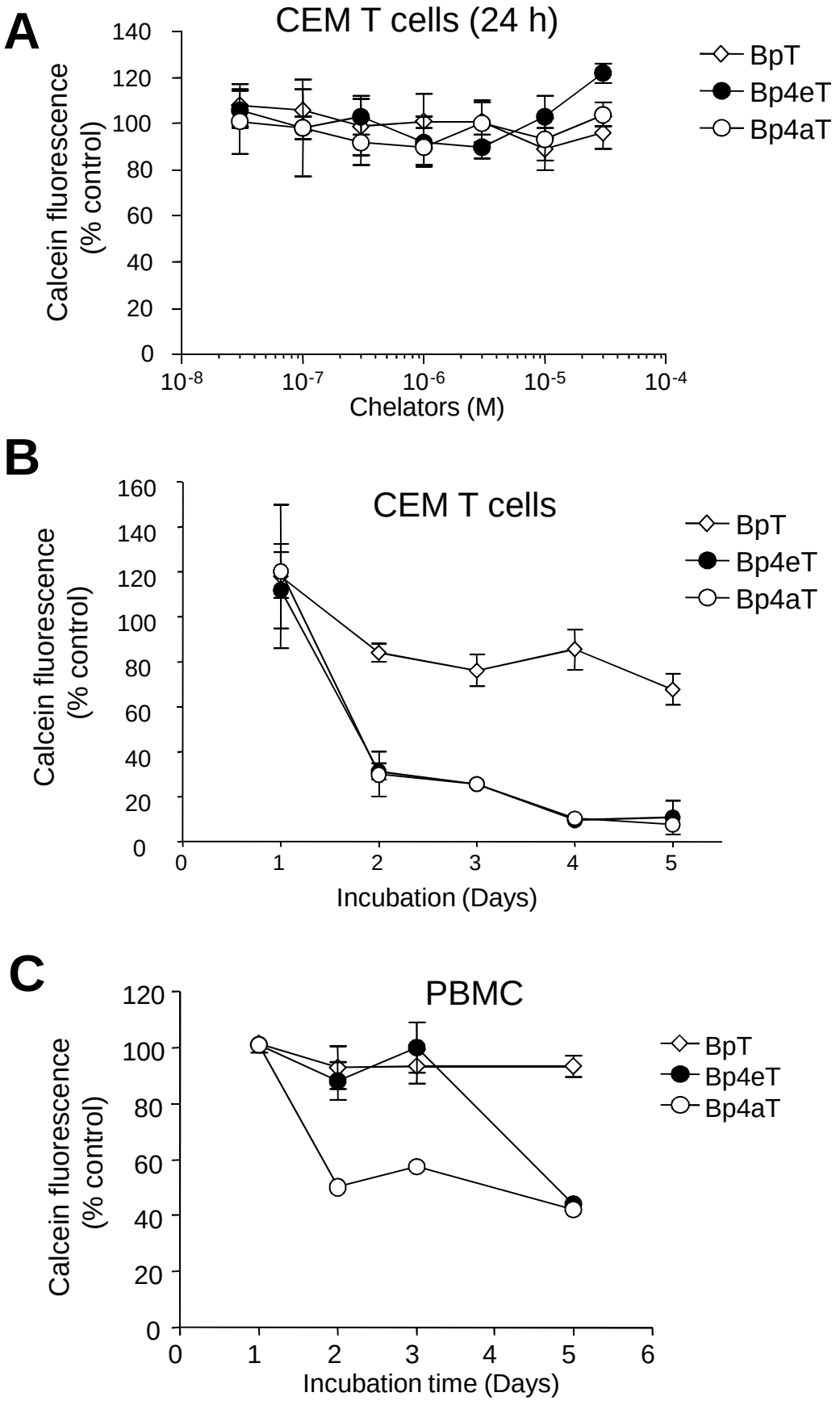

Figure 4

Molecular Pharmacology Fast Forward. Published on October 18, 2010 as DOI: 10.1124/mol.110.069062
This article has not been copyedited and formatted. The final version may differ from this version.

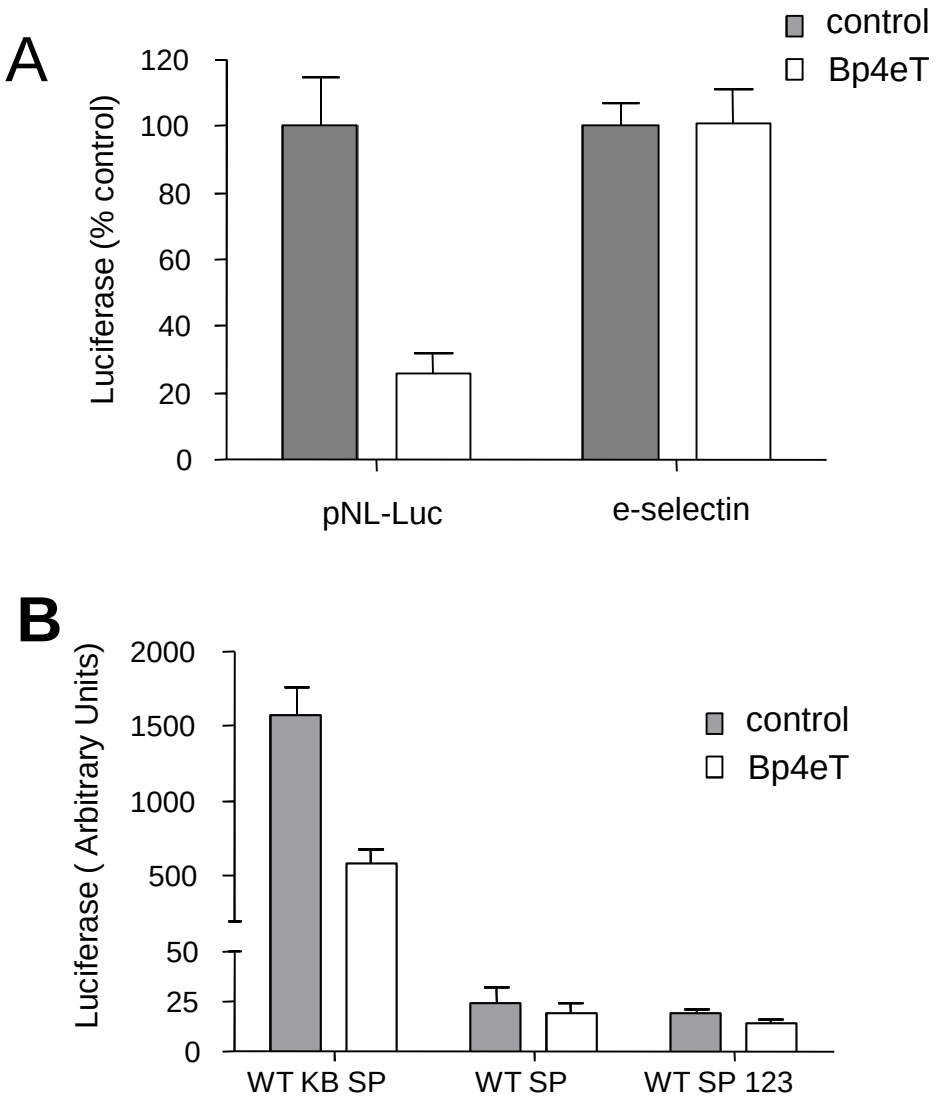

Figure 5

Molecular Pharmacology Fast Forward. Published on October 18, 2010 as DOI: 10.1124/mol.110.069062
This article has not been copyedited and formatted. The final version may differ from this version.

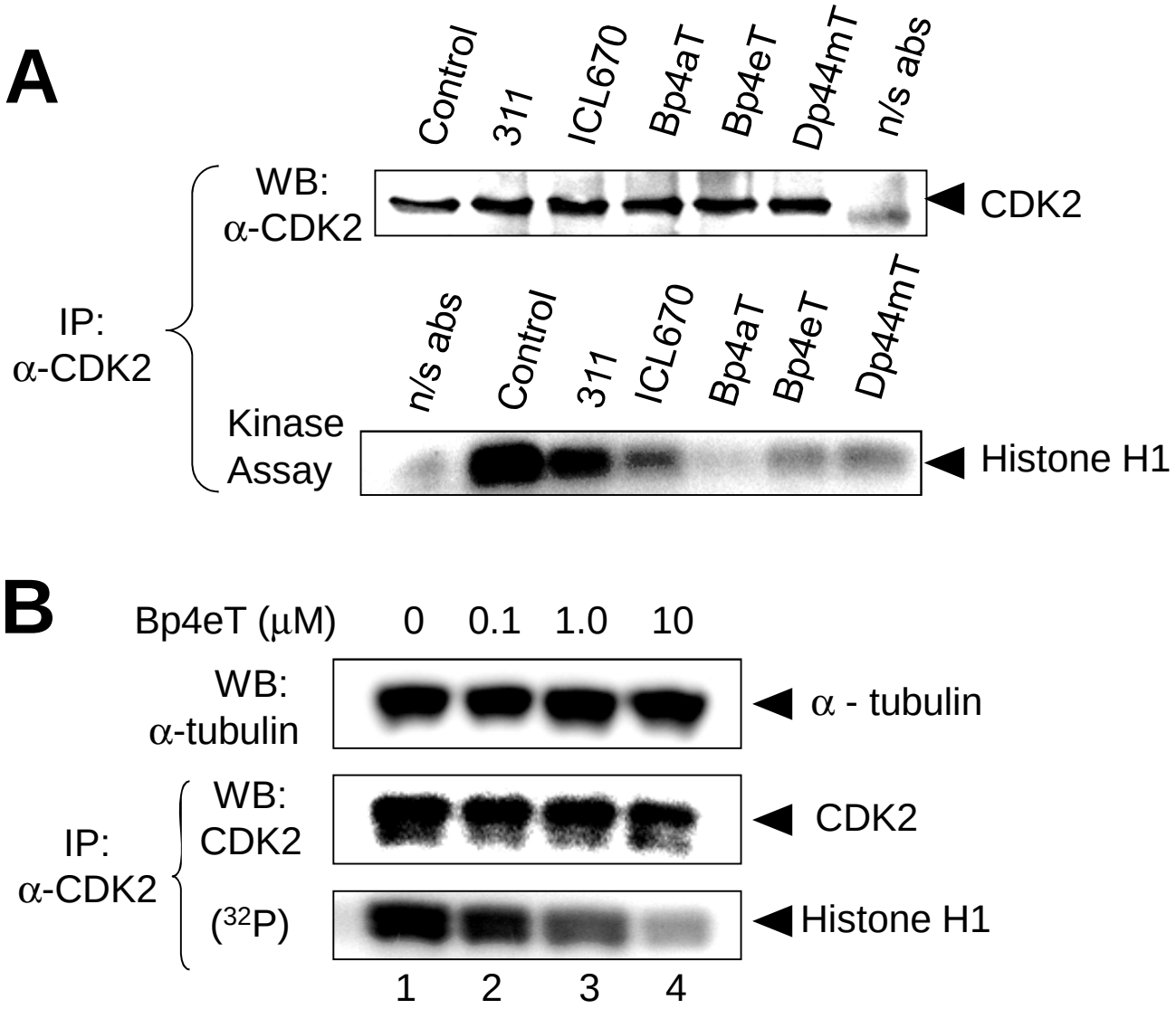

Figure 6

Molecular Pharmacology Fast Forward. Published on October 18, 2010 as DOI: 10.1124/mol.110.069062
This article has not been copyedited and formatted. The final version may differ from this version.

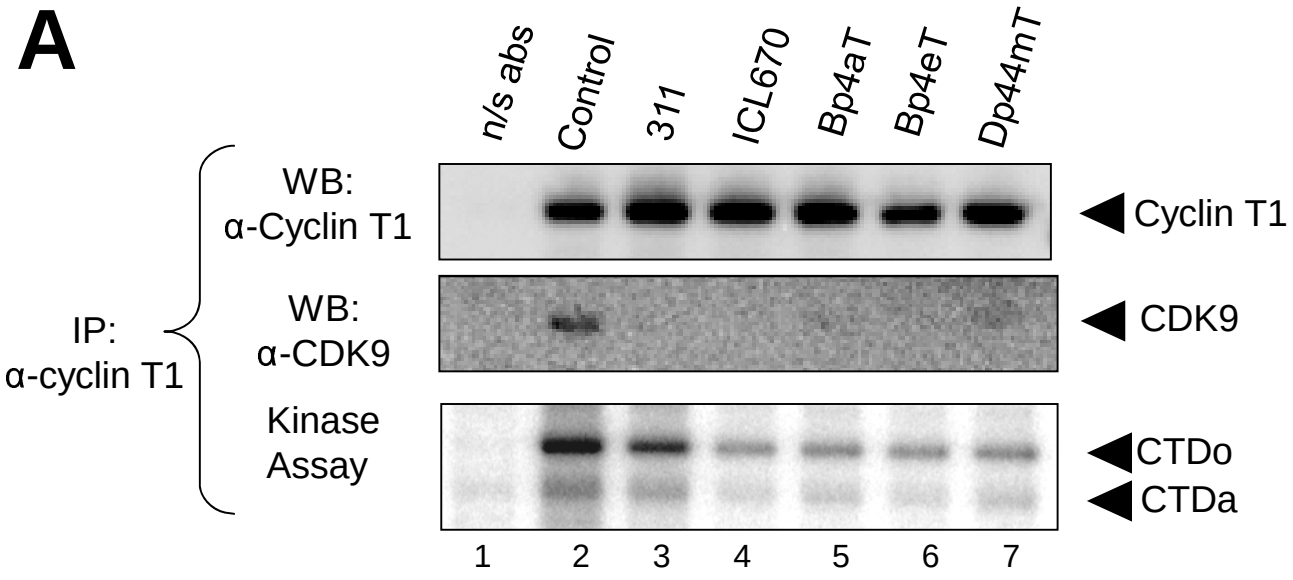

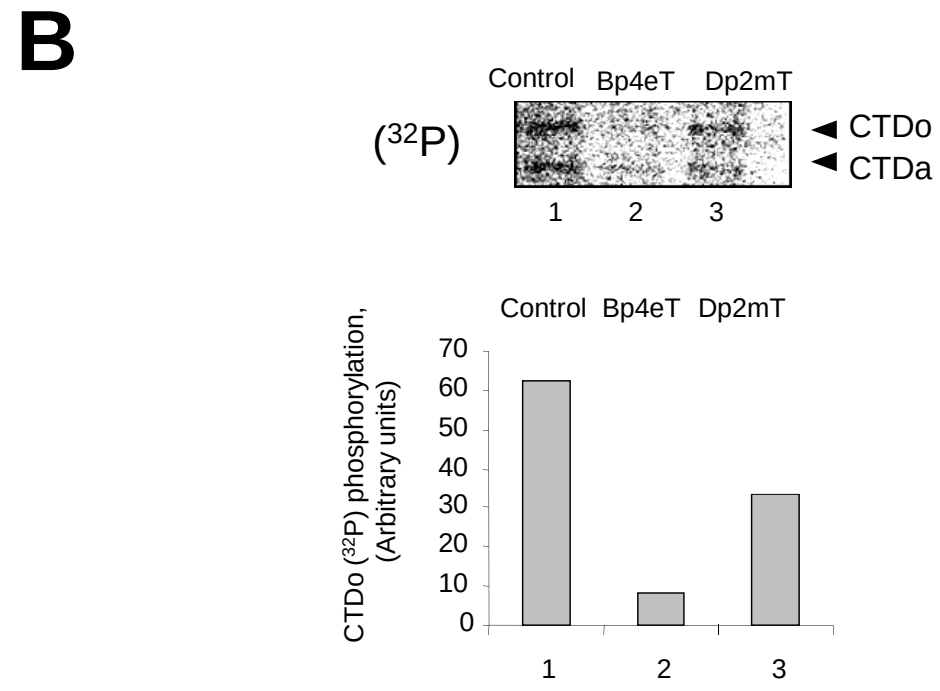

Figure 7

Molecular Pharmacology Fast Forward. Published on October 18, 2010 as DOI: 10.1124/mol.110.069062
This article has not been copyedited and formatted. The final version may differ from this version.

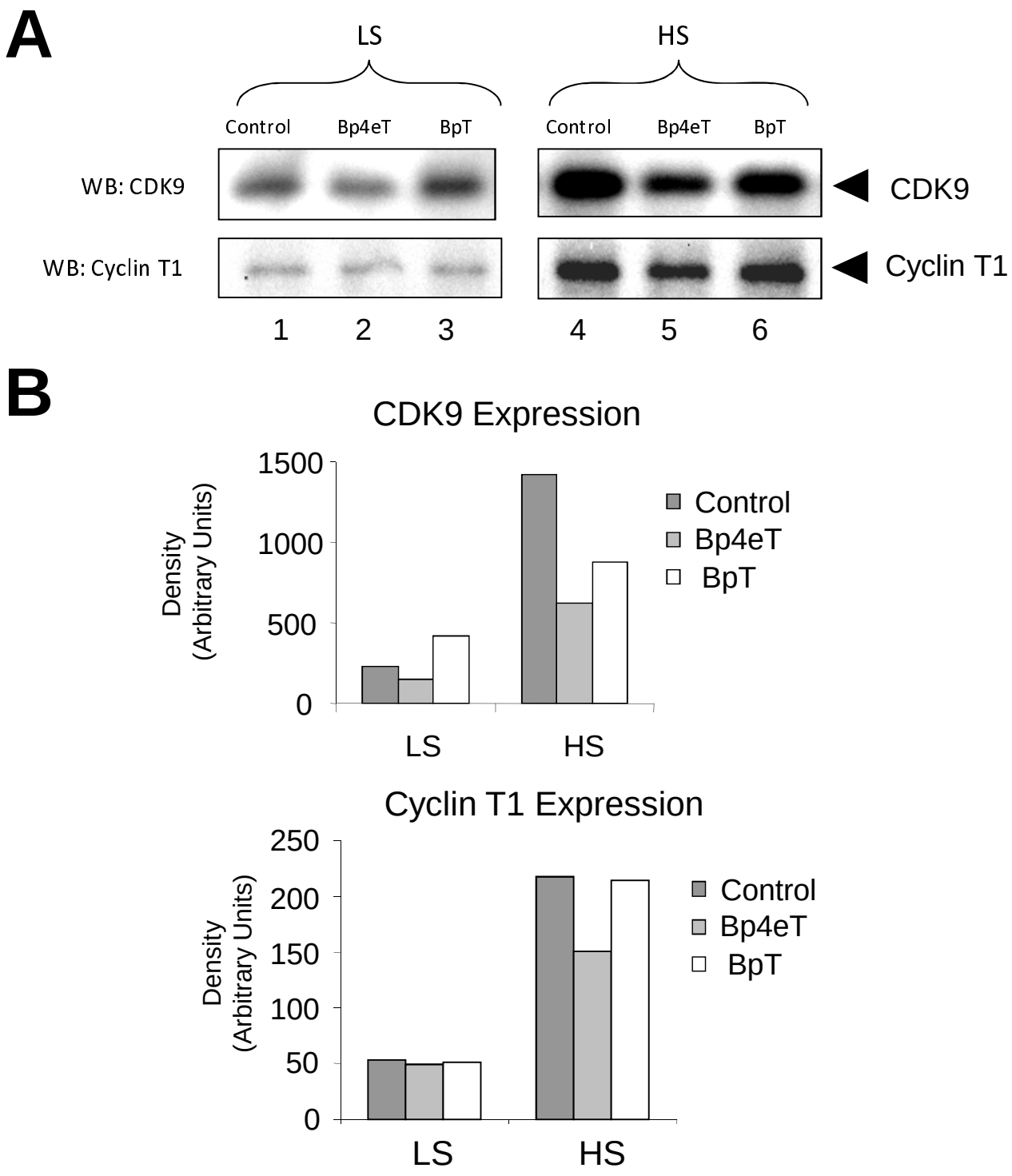

Figure 8